Int J Clin Exp Med 2019;12(6):6671-6683
www.ijcem.com /ISSN:1940-5901/IJCEM0088518

Original Article

Squamous cell carcinoma of the lung: gene expression and network analysis during carcinogenesis

Angel Juarez-Flores[1,2], Marco V José[2]

[1]*Posgrado en Ciencias Biológicas, Unidad de Posgrado, Circuito de Posgrados, Ciudad Universitaria, Universidad Nacional Autónoma de México, CP 04510, Mexico City, Mexico;* [2]*Theoretical Biology Group, Instituto de Investigaciones Biomédicas, Universidad Nacional Autónoma de México, CP 04510, Mexico City, Mexico*

Received October 31, 2019; Accepted March 12, 2019; Epub June 15, 2019; Published June 30, 2019

Abstract: Lung cancer is one of the most common and deadliest types of cancer. Most often, diagnosis is made in the later stages of the disease, with few treatment options available. Squamous cell carcinoma of the lung (SCCL) is one of the most common types of lung cancer. Knowledge concerning its carcinogenic process lags behind that of other cancers of the lungs. Aiming to understand the biological phenomena underlying each stage of the disease and unveil the most significant genes, the current study carried out bioinformatic analysis of different samples that corresponded to the carcinogenic process. New relevant genes for early diagnosis and treatment are proposed and expression profiles for each stage are presented. Based on Protein-Protein interaction networks of these genes, this study proposes that they function as gatekeepers for a wide variety of processes. MYC, MCM2, AURKA, CUL3, and DDIT4L are proposed as a possible group for treatment of SCCL. This work provides a general panorama of the transcriptome profile of SCCL, with a plethora of information regarding its carcinogenesis. Results obtained by this *in silico* approach constitute a guide for further experimental works necessary for corroborating and validating their potential application for diagnosis and treatment of the disease.

Keywords: Squamous lung cancer, carcinogenesis, microarray, carcinoma, transcriptome

Introduction

In 2018, statistical epidemiological estimates showed that lung cancer is one of the most frequent and deadliest types of cancer, worldwide, even in developed countries. For both sexes, statistics showed 2,093,876 new cases and 1,761,007 deaths [1, 2]. Lung cancer is commonly divided into two types, small cell lung cancer (SCLC) and non-small cell lung cancer (NSCLC). NSCLC comprises approximately 85% of all lung cancers [3, 4]. NSCLC adenocarcinoma and squamous cell carcinoma (SCC) of the lungs are the most prevalent [5, 6]. However, cancer therapies mostly focus on treatment of adenocarcinoma. Incidence of adenocarcinoma has increased in recent years [5]. In most patients, cancer diagnosis is made in late stages when metastasis is often present and available treatments are not as effective [7]. Surgery is the best treatment option, but only in the earlier stages of the disease. Available therapies for advanced stages are limited. There has been little improvement observed in patient survival. Standard treatment consists of platinum-based doublet therapy [7, 8]. Squamous cell carcinoma of the lungs is mainly associated with cigarette smoking [5]. Its carcinogenic process is described by different stages. The first step is hyperplasia, followed by metaplasia, varying degrees of dysplasia, and carcinoma *in situ*, finally reaching squamous cell carcinoma [6, 9]. Histology is the main criterion in classifying stages of carcinogenesis. Some chromosomal losses appear in the process [6]. A better understanding of pre-disease and early events that occur during the carcinogenic process will assist in improving early diagnosis and achieving better outcomes. The current study consists of transcriptome profiling, with enrichment and network analysis as an aid, aiming to better understand the carcinogenic process of SCC. This study highlights genes with the most statistically significant expression. Underlying

biological processes for each stage are described with the help of gene ontology. This study also used a Protein-Protein interaction (PPI) network to highlight some proteins with a high number of connections.

Materials and methods

Data retrieval

A search was conducted in the National Center for Biotechnology Information Gene Expression Omnibus database, retrieving the following datasets: Squamous cell carcinoma, GEO accession: GSE33479, with 122 samples which represent carcinogenic stages. The samples were divided, including 13 with normal histology and normofluorescence and 14 with normal histology and hypofluorescence. They were selected as the control group, including 15 for metaplasia, 13 for mild dysplasia, 13 for moderate dysplasia, 12 for severe dysplasia, 13 for carcinoma *in situ*, and 14 for squamous cell carcinoma of the lungs. The platform was: Agilent-014850 Whole Human Genome, Microarray 4x44K G4112F. All analyses were performed using *R* v3.4.3 software (http://www.R-project.org).

Differential gene expression analysis

First, this study obtained preprocessed data from the SOFT file, according to the manual of the *GEOquery* R package and *hgug4112a.db* R package was used to annotate each gene ID to the data [10]. Differential gene expression (DGE) analysis was performed, making a comparison of each stage against the control using the *limma* package. It fits a generalized linear model before comparisons and calculates a moderate t-statistic for each contrast [11, 12]. A *p*-value was obtained. It was adjusted based on the Benjamini and Hochberg False Discovery Rate correction using *limma* [11, 13]. Volcano plots were constructed for each cancer stage, in which upper left and upper right points in the plot were selected genes that fulfilled a double criterion: False Discovery Rate (FDR) adjusted p-value < 0.05 and a Fold Change value > 1.5 or < -1.5.

Gene ontology enrichment analysis

Gene Ontology (GO) enrichment analysis was performed with the topGO package (http://bioconductor.org/packages/topGO/) as follows: As the gene universe, all of the genes contained in the Agilent chip and *hgug4112a.db* library were used for annotation. Relevant genes were the ones showing an FDR adjusted p-value < 0.05. Statistical testing for *topGO* classic Fisher, classic Kolmogorov-Smirnov (KS), and a variation of KS (elimKS) available in the *topGO* program, was conducted. Classic Fisher is based on gene counts. It is related to hypergeometric probability, rendering a p-value of the overlap between two independent sets. In the topGO version, it uses modular enrichment analysis (MEA), which considers inter-relationships of GO terms. The list of relevant genes was input [14, 15]. Classic K-S and elimKS are based on gene scores, providing Gene set enrichment analysis which reduces arbitrary factors and uses all information of the microarray. They use scores (p-values) obtained from DGE analysis as input. Moreover, elimKS is a more conservative KS variation [14, 15]. More enrichment analysis was made using *PANTHER* v13.1 (PANTHER Enrichment Test Released 201704-13). Input data were the list of selected genes by the volcano plots (double criteria). Gene Universe was the database default for *Homo sapiens*, using the complete GO annotation dataset provided by the software (GO Ontology Database Released 2018-09-06) [16]. Selected analysis for *PANTHER* was statistical overrepresentation enrichment testing. The test type was Fisher's exact test, with FDR multiple test correction. This study compared the results of *topGO* and *PANTHER*, finding common *GO* enriched terms in each stage, except for hyperplasia. No statistical differences were found with *limma* and the normal stage (used as control), according to differential gene expression analysis.

Network construction and analysis

For this study, researchers downloaded the full interactome of *Homo sapiens* from Mentha database [17]. Retrieval, construction, management, and network analysis of the PPI were made with Cytoscape software. Retrieved interactions were curated by the database, which only integrates data from experimentally determined direct protein interactions [18]. For network construction, duplicated edges (lines that bind nodes), nodes (ellipses that represent a protein), and self-loops were deleted to create an interactome network, functioning as a basic template. Network Analyzer was used to calculate the number of connections for each node

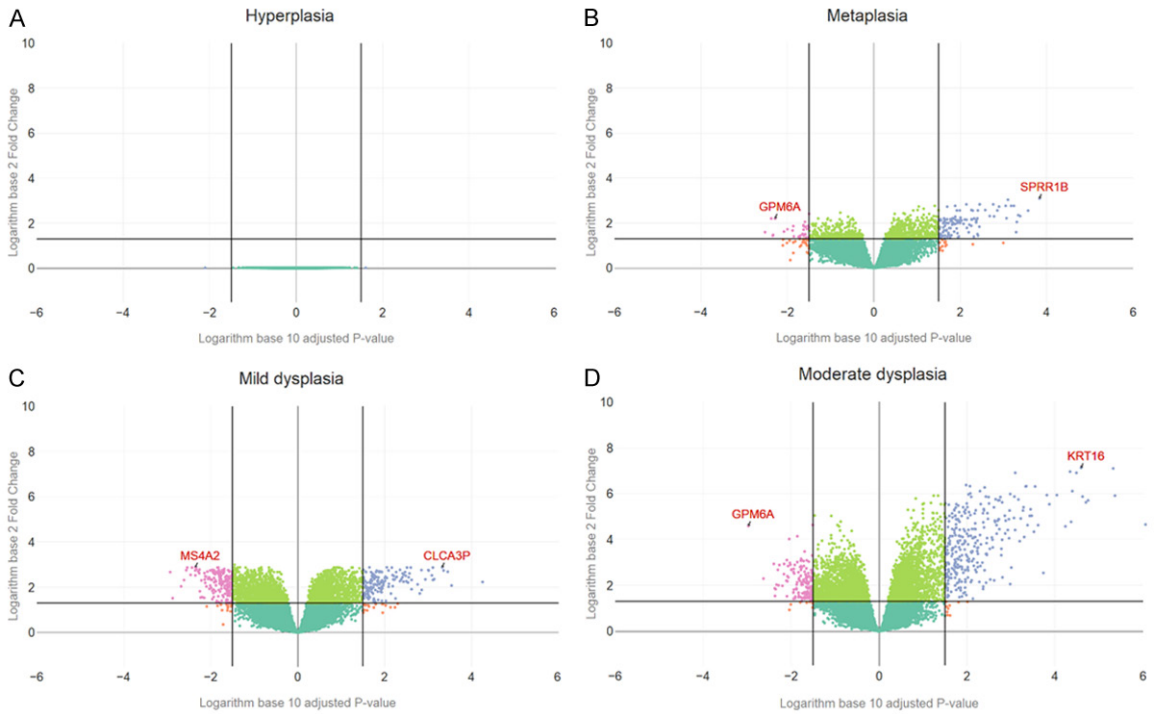

Figure 1. Volcano plots. (A) Hyperplasia; (B) Metaplasia; (C) Mild dysplasia; (D) Moderate dysplasia. Two genes with FC > 1.5 and the minor *p*-value are selected were tagged with their respective names in each cancer stage. Vertical lines divided the genes by FC criteria > 1.5 to the right (over expressed) or < -1.5 to the left (down expressed). The black horizontal line is the *p*-value cutoff: above the line < 0.5, in the line = 0.05, down the line > 0.05.

[19]. Networks with the first neighbors of some of the highlighted genes in the Volcano plots were retrieved from the basic template network, creating a graphical network output for each node. The size represents the number of connections they had in the original template. Next, generated lists of all the genes selected by the double filter criteria in all stages were merged. Duplicated genes were deleted, creating a single list with 2,199 genes. This list was used to find matches with the created interactome network, with 1,793 genes identified. Nodes that matched the previous list were selected to create a new network. Some nodes had no connections. Thus, it was processed to eliminate these nodes, creating a unique network in which every node was connected. This study obtained a final network with 1,152 nodes. For every node in the final network, Network Analyzer was used to calculate the degree, number of connections of each node, and betweenness. This is a measure based on the shortest paths (the short path from a point a to a point b), indicating that it is a measure of highest number of times that a node is passed by the shortest paths [20].

Results

First, differential gene expression analysis was conducted, using double criteria calculated from the volcano plots for every stage of the carcinogenic process. **Figures 1A-D** and **2A**, **2B** show the so-called pre-disease stages. In **Figure 2C**, the cancer stages are shown. As stages become more advanced, the number of significant genes increases (both by fold change and statistical *p*-value (see **Figure 2D** for a better understanding), indicating greater alterations in expression profiles patterns, according to the advancement of the disease. This could indicate a necessity of the cells for new processes to be upregulated or downregulated, depending on the requirements for its development and potential outcomes of cancer stage and metastasis. An example is the case of metalloprotease proteins, which were detected in the moderate dysplasia stage (See Table S1 in Supplementary Information at the end of the paper), upregulated (data not shown) with the highest number of them in the carcinoma *in situ* and squamous cell carcinoma stages. Expression profiles for each stage were found

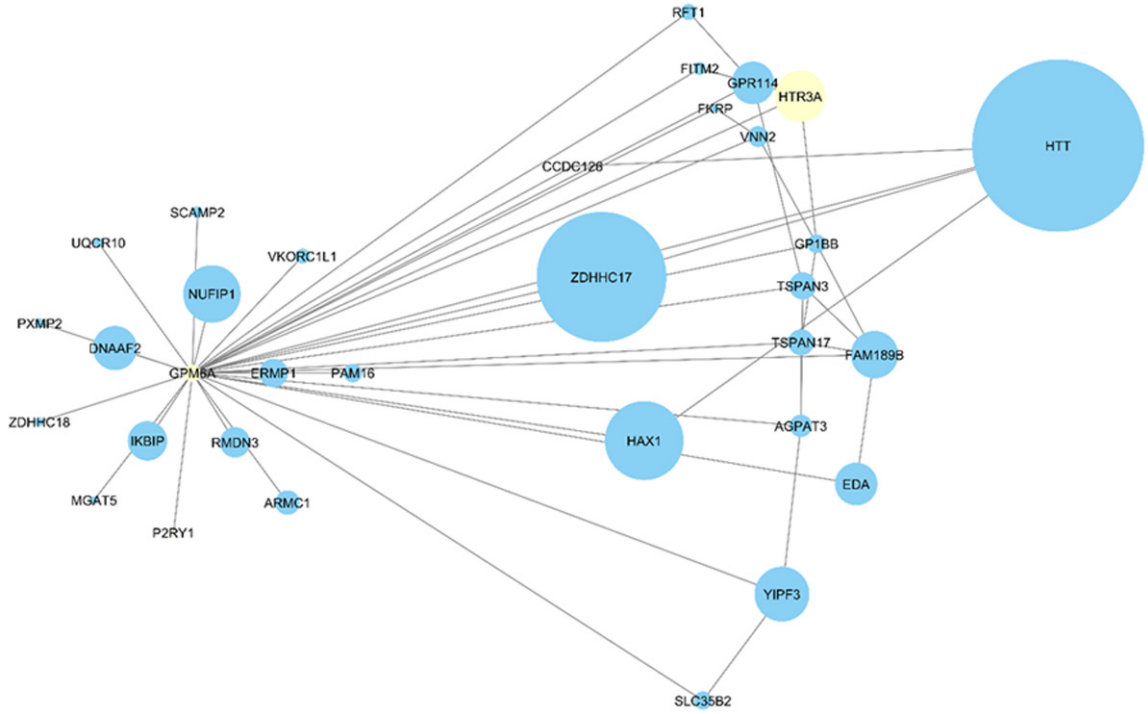

Figure 2. GPM6A network. This graph shows the first neighbors nodes that are connected to GPM6A. The size of the nodes is related to the number of connections they had in the base network. Nodes in yellow color are the ones that are in the list created using the double filter criteria. HTT is the most connected node that interact directly with GPM6A.

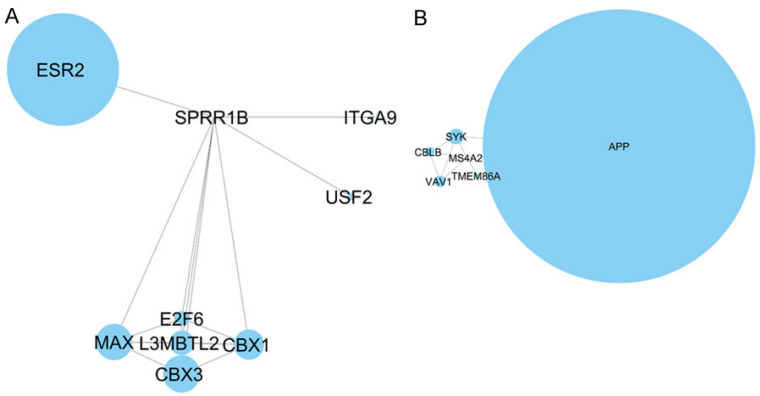

Figure 3. SPRR1B and MS4A2 networks. A: Shows the first neighbors nodes that are connected to SPRR1B; ESR2 is the most connected node. B: Shows the first neighbors nodes that are connected to MS4A2; APP is the most connected node. The size of the nodes is related to the number of connections they had in the base network.

and presented in Table S1, which corresponds to the genes with a differential expression. For each stage, two genes are pointed out using an arrow with their respective names, except for the hyperplasia stage, which shows no statistical significance.

In **Figure 1**, selected genes for each stage (except for hyperplasia) are: a) Metaplasia: GPM6A-This is a protein involved with neural differentiation. It may be involved in regulation of endocytosis and intracellular trafficking of G-protein-coupled receptors. Thus far, it has not been associated with cancer [21]; SPRR1B-This is an envelope protein with transglutaminase cross-linking properties of keratinocytes. It can function as an amine donor and acceptor in transglutaminase-mediated cross-linkage. It has been proposed as a biomarker for squamous metaplasia and oral squamous cell cancer stem-like cells. It has also been suggested that its upregulation suppresses RASSF4, a tumor suppressor [22-25]; b) Mild dysplasia: MS4A2-This is a high affinity receptor that binds to the Fc region of immunoglobulins

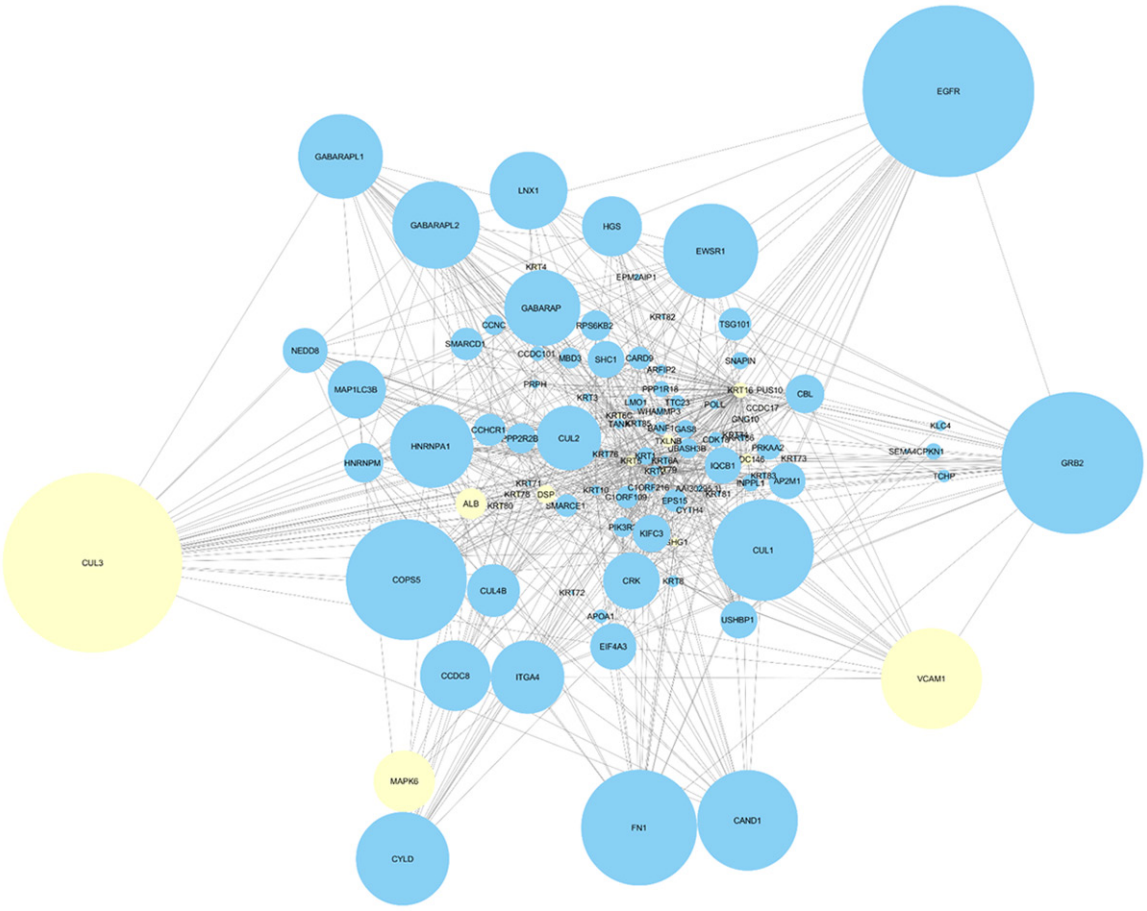

Figure 4. KRT16 network. Shows the first neighbors nodes that are connected to KRT16. The size of the nodes is related to the number of connections they had in the base network. Nodes in yellow color are the ones that are in the list created using the double filter criteria. CUL3 and EFG3 are the most connected nodes that interact directly with KRT16.

epsilon. It can mediate the secretion of some lymphokines. In adenocarcinoma, it has been suggested that its expression is an independent prognostic marker for patient survival [26-28]; CLCA3P-This is a pseudogene. When it is cloned and expressed, it produces a protein that is secreted into the culture supernatant, but no function has yet been ascribed [29]; c) Moderate dysplasia: GPM6A, KRT16-This is a keratin protein that could act as a regulator of innate immunity in response to skin barrier breach. In oral squamous cell carcinoma, it is overexpressed. In metastatic breast cancer, it is associated with a shorter relapse-free survival [30-32]. Although **Figures 3-5** shows that GPM6A, SPRR1B, and MS4A2 had few interactions, proteins that were connected to them had plenty of interactions. Thus, they seem to function as "gatekeepers" for a wide variety of processes. KRT16 had more direct interactions than others. It also had interactions with highly connected proteins, as seen in **Figure 4**.

In **Figure 2**, selected genes included: a) Severe dysplasia: HSD17B13-This is a member of the hydroxysteroid 17-beta family. Its function is unknown. Overexpression in mice and cultured hepatocyte lines increases lipogenesis. In hepatocellular carcinoma, its downregulation has been associated with worse survival in patients [33, 34]. KRT6B-This is a member of the keratin gene family and a type II cytokeratin. It has been suggested that its upregulation might contribute to renal cell carcinoma progression [35, 36]; b) Carcinoma *in situ*: ASXL3-This is a putative polycomb group protein. It acts by forming multiprotein complexes to maintain a repressive state in lung induced-pluripotent stem cells. Its silencing has inhibited proliferation and diminished malignant

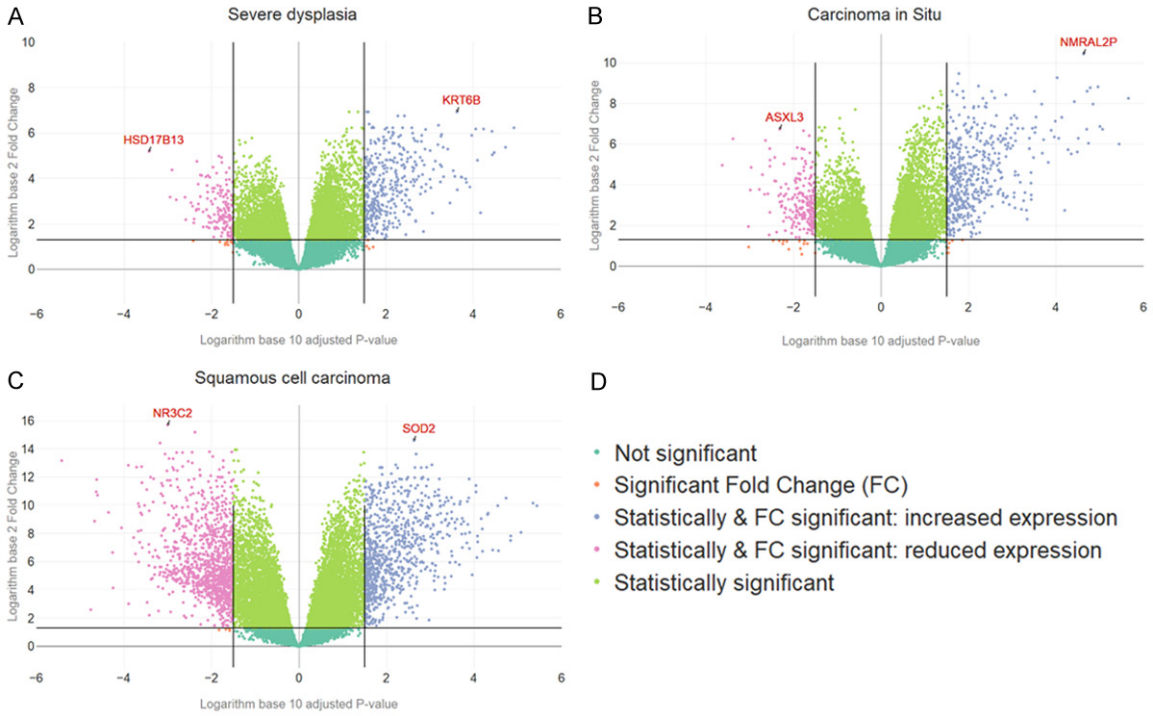

Figure 5. Volcano plots (continuation). (A) Severe dysplasia; (B) Carcinoma *in situ*; (C) Squamous cell carcinoma of the lungs; (D) Color codes. The two genes with FC > 1.5 and the minor *p*-value are selected and tagged with their respective names in each cancer stage. Vertical lines divided the genes by FC criteria > 1.5 to the right (over expressed) or < -1.5 to the left (down expressed). The black horizontal line is the *p*-value cutoff: above the line < 0.5, in the line = 0.05, down the line > 0.05.

growth in small cell lung cancer cells. Thus, it was proposed to be a novel candidate target for therapy [37, 38]; NMRAL2P-This is a pseudogene. It has been identified as a direct transcriptional target of Nrf2 in colon cancer cell lines [39]; c) Squamous cell carcinoma of the lungs: NR3C2-This is a mineralocorticoid receptor. It binds to mineralocorticoid response elements and transactivates target genes. Reduced levels of expression have correlated with poorer survival in pancreatic ductal adenocarcinoma [40, 41]; SOD2-This is a superoxide dismutase which destroys superoxide anion radicals. It was observed to have tumor suppressive and promoting functions [42, 43]. **Figures 6-8** show connections at the first neighbor level for highlighted proteins (**Figure 5**). Except for HSD17B13 (**Figure 6**), the proteins had interactions with highly connected proteins. KRT6B and KRT16 had the most direct interactions.

To gain further insight concerning the underlying processes, this study conducted enrichment analysis with different methods, using two different software platforms. Results were compared to found matches, as summarized in **Table 1**. **Table 1** only shows the results that matched between topGO and PANTHER. In **Table 2**, some cancer stages for GO molecular function and cellular component did not have a match between topGO and PANTHER. Thus, only topGO principal results are used in **Tables 2** and **3** (see caption). In GO biological process (BP) (**Table 1**), cell division was found to be important in four stages between metaplasia to carcinoma *in situ* (except mild dysplasia). Cornification was also found in the four stages, which could mean that this process starts early in the carcinogenic process. DNA replication initiation was found in two stages (moderate and SCC) and sister chromatid cohesion was found in two stages (moderate and severe dysplasia). **Table 2** shows GO molecular function (MF). Protein binding was found in the four stages from moderate dysplasia to squamous cell carcinoma. **Table 3** shows GO cellular components (CC). Cytosol and condensed chromosome outer kinetochore were found in all stages, except for mild dysplasia. Extracellular exosome was encountered in mild dysplasia and squamous cell carcinoma.

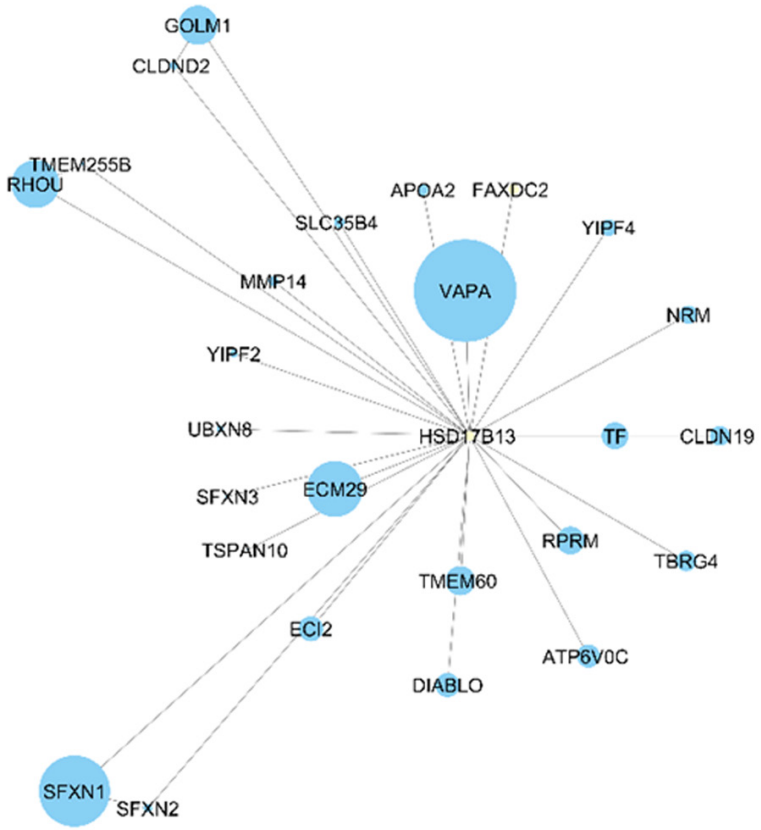

Figure 6. HSD17B13 network. The first neighbors nodes that are connected to HSD17B13 are shown. The size of the nodes is related to the number of connections they had in the base network. VAPA is the most connected node that interacts directly with HSD17B13.

A network was created. Components were the protein products of genes that were selected by the double filter criteria. This study calculated degrees (number of connection) and betweenness using the Network Analyzer. In **Table 4**, the top five nodes for each measure, in descending order, are shown. They may play important roles in SCCL development: MYC (found upregulated in this work) is a transcription factor that promotes angiogenesis trough VEGFA. Its upregulation could promote esophageal squamous cell carcinoma [44, 45]; MCM2 (upregulated) and AURKA (upregulated) participate in cell cycle regulation [46, 47]. MCM2 deregulation was found to be involved in lung cancer cell proliferation [48]; AURKA has been found to be overexpressed in oral squamous cell carcinoma cells. Its suppression inhibits cancer growth [49]; CUL3 (downregulated) participates in ubiquitination and proteasomal degradation. When silent in breast cancer, it makes cell lines more resistant to treatments, such as doxorubicin and paclitaxel [50, 51]; DDIT4L (downregulated) acts as an inhibitor of mTOR signaling. It was found that its downregulation promotes cutaneous SCCL proliferation [52-54]. These proteins may also function as an axe of regulation, due to high connectivity and the short paths that pass through them. However, the genes previously highlighted are not in the list of top nodes, but they are biologically relevant.

Discussion

During analysis, a wide variety of genes with a significant change of expression were detected. This study points out some of them, denoting the possible importance of their expression during the carcinogenesis process of squamous cell carcinoma of the lungs. Most of the highlighted genes have been reported in other types of cancer [22, 26, 30, 31, 35, 39, 43]. Only CLCA3P, which is a pseudogene, had not been reported in cancer. Its function remains unknown [29]. Occurring with other types of cancers, genes SPRR1B, KRT16, KRT6B, and NMRAL2P were found via the double filter criteria to be significant in the carcinogenesis process (except hyperplasia). Upregulation of these genes has been associated with cancer promotion or patient poor survival [22, 30, 31, 35, 39]. GP6MA was found to be significant in the carcinogenesis process. It is downregulated, but it has not yet been associated with cancer. Since GP6MA is related with G-protein-coupled receptors, it could play an important role in SCC promotion. The latter, together with the above-mentioned genes, may play a role as early biomarkers for SCC. Expression patterns of the highlighted genes matched those observed in other types of cancers. Therefore, they should participate as cancer promoter-genes beginning at precancerous stages, making them potentially useful as therapeutics targets. In this list of highlighted genes, there were

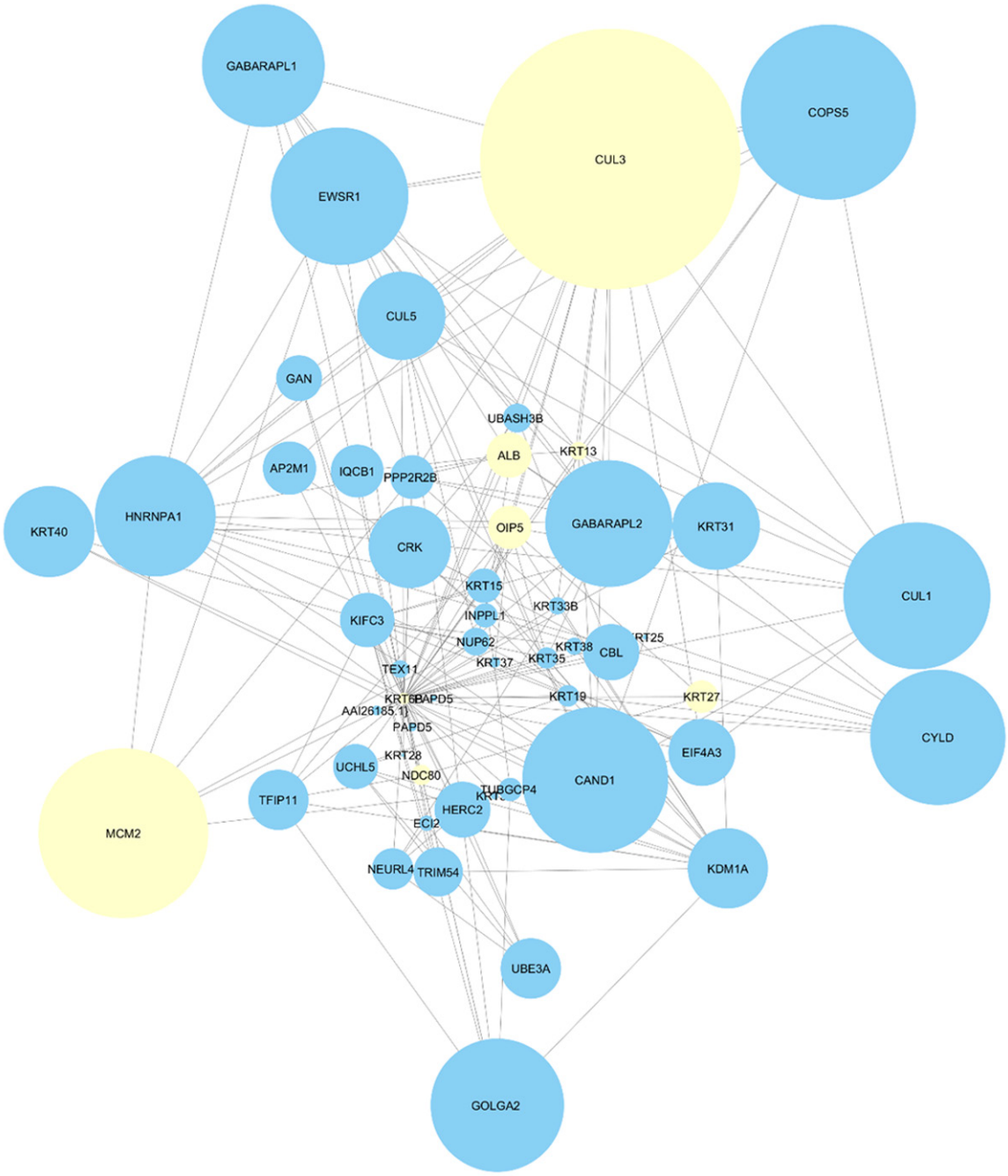

Figure 7. KRT6B network. The first neighbors nodes that are connected to KRT6B are displayed. The size of the nodes is related to the number of connections they had in the base network. Nodes in yellow color are the ones that are in the list created using the double filter criteria. CUL3 is the most connected node that interact directly with KRT6B.

others, like HSD17B13 and CLCA3P, with expression levels found to be significant since the mild dysplasia stage, including SOD2 since the carcinoma *in situ* stage, ASXL3 since the severe dysplasia stage, and NR3C2, only in the cancer stage. Only MS4A2 was found to be significant both in mild dysplasia and moderate dysplasia stages. Some upregulated genes were identified as part of the keratin family. This is a family of structural proteins. In preinvasive lesions, this study found two types of keratins that were upregulated (**Figures 1**, **2**).

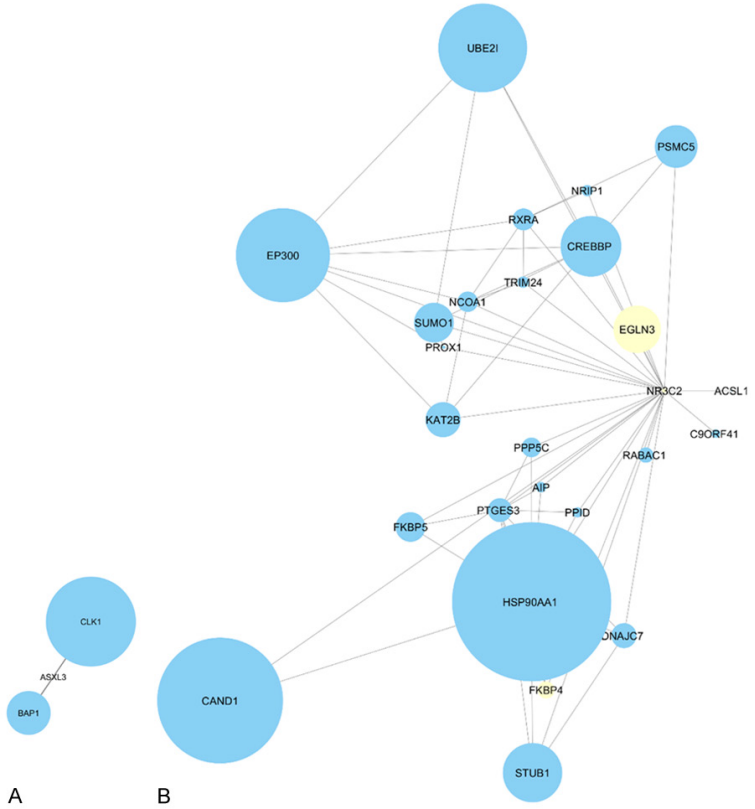

Figure 8. ASXL3 and NR3C2 network. A: Shows the first neighbors nodes that are connected to ASXL3. The size of the nodes is related to the number of connections they had in the base network. CLK1 is the most connected node that interact directly with ASXL3; B: The first neighbors nodes that are connected to NR3C2 are shown. The size of the nodes is related to the number of connections they had in the base network. Nodes in yellow color are the ones that are in the list created using the double filter criteria. HSP90AA1 is the most connected node that interact directly with NR3C2.

As mentioned before, these proteins do not have much interaction, compared to other proteins (**Figures 3**-**8**). However, since they are connected to highly connected ones, they are likely to function as gatekeepers in a wide variety of signaling process. Networks are useful in supporting and visualizing results of volcano plots. These plots assist in observing details of how the highlighted genes are connected. Centrality measures, such as degrees and betweenness of the network, are useful in finding some proteins that had significant importance. However, this analysis only provides a glimpse of the full panorama of what is happening biologically. The full panorama is obtained with network analysis, combined with volcano plots. According to GO analysis, it was found that the cornification process, which is a type of cell death, was significant in some stages [9, 55]. Also, a portion of the genes related to the cornification process was found to have a significant change in expression values, beginning at the earliest moment of the carcinogenesis process (data not shown). This suggests that they could be necessary in reaching the cancer stage. Subsequent development may be in a way, similar to that which occurs with KRT6B and KRT16 in renal cell carcinoma and breast cancer, respectively [30, 35]. Another process that was pointed out by enrichment analysis was cell division. This was expected due to the constant cell division in cancer cells. A very important portion in the number of genes was found to be significant. However, there were none in the ones selected for volcano plots. MYC, MCM2, AURKA, CUL3, and DDIT4L were found by DEG analysis. GO enrichment analysis showed that the processes in which they participate are relevant in various stages. Network analysis also found them as important participant proteins in the networks of the DEG. Thus, it is proposed that they should be studied as a group of proteins for possible combined multi-target treatment of SCCL. Some processes and genes that are upregulated or downregulated were detected, beginning with the earliest moments of the carcinogenic process. They continued to the last stages of the process, suggesting importance not only in cancer *per se* but also in pre-disease stages. This could also be the case for KRT16. KRT16 expression was different and statistically significant, beginning at metaplasia all the way to SCCL. Further experimentation is necessary to validate the genes proposed in this study, determining whether they are also useful in finding unknown functions of the carcinogenic process.

Conclusion

The current study identified genes that may herald the development of squamous cell carcinoma of the lungs. These genes were shown

Table 1. GO Biological process similarities between topGO and PANTHER for each stage of squamous lung cancer

Biological Process					
Metaplasia	Mild dysplasia	Moderate dysplasia	Severe dysplasia	Carcinoma in situ	Squamous cell carcinoma
Cell division (GO: 0051301)	Cornification (GO: 0070268)	Cell division (GO: 0051301)	Sister chromatid cohesion (GO: 0007062)	Anaphase-promoting complex-dependent catabolic process (GO: 0031145)	Neutrophil degranulation (GO: 0043312)
Cornification (GO: 0070268)		Cornification (GO: 0070268)	Cell division (GO: 0051301)	Cell division (GO: 0051301)	DNA replication initiation (GO: 0006270)
		Sister chromatid cohesion (GO: 0007062)	Cornification (GO: 0070268)		Anaphase-promoting complex-dependent catabolic process (GO: 0031145)
		DNA replication initiation (GO: 0006270)	Anaphase-promoting complex-dependent catabolic process (GO: 0031145)		

Table 2. GO Molecular function similarities between topGO and PANTHER for each stage of squamous lung cancer

Molecular function*					
Alditol: NADP+ 1-oxidoreductase activity (GO: 0004032)	Extracellular matrix structural constituent (GO: 0005201)	Structural constituent of muscle (GO: 0008307)	Phosphatidic acid transporter activity (GO: 1990050)	Protein binding (GO: 0005515)	Protein binding (GO: 0005515)
	Platelet-derived growth factor binding (GO: 0048407)	Protein binding (GO: 0005515)	ATP binding (GO: 0005524)		RNA binding (GO: 0003723)
		Cadherin binding (GO: 0045296)	Protein binding (GO: 0005515)		Dynein light chain binding (GO: 0045503)
					Microtubule motor activity (GO: 0003777)

*In molecular function, there were no matches between topGO and PANTHER but they were found in Metaplasia, Moderate dysplasia, and Severe dysplasia.

Table 3. GO Cellular component similarities between topGO and PANTHER for each stage of squamous lung cancer

Cellular component*					
Cytoplasm (GO: 0005737)	Extracellular exosome (GO: 0070062)	Cytosol (GO: 0005829)	Cytosol (GO: 0005829)	Cytosol (GO: 0005829)	Extracellular exosome (GO: 0070062)
Condensed chromosome outer kinetochore (GO: 0000940)		Condensed chromosome outer kinetochore (GO: 0000940)	Condensed chromosome outer kinetochore (GO: 0000940)	Condensed chromosome outer kinetochore (GO: 0000940)	Condensed chromosome outer kinetochore (GO: 0000940)
Cytosol (GO: 0005829)		Centrosome (GO: 0005813)	Condensed chromosome kinetochore (GO: 0000777)	Cornified envelope (GO: 0001533)	Spindle microtubule (GO: 0005876)
					Nucleoplasm (GO: 0005654)
					Tertiary granule membrane (GO: 0070821)

*In Cellular components, no matches found between topGO and PANTHER with Metaplasia.

Table 4. Top nodes in the final PPI network

Top nodes for Betweenness	Top nodes for Degree*
MYC	MYC
DDIT4L	DDIT4L
MCM2	MCM2
CUL3	CUL3
AURKA	CDK1

*Most of the top nodes were shared between the degree and betweenness measures.

to be involved in keratinization and cornification processes. This study also identified individual genes, previously reported in many types of cancer, that are relevant in the processes of growth, metastasis, and cell division. Network analysis results suggest that these genes could function as gatekeepers for a wide variety of signaling processes. Likewise, some processes were expected to be relevant, including cell division or DNA replication initiation. This work provides a general panorama of the transcriptome profile of squamous cell carcinoma of the lungs, contributing a wealth of information concerning its carcinogenesis. Results obtained from this *in silico* approach constitute a guide for further experimental works. Future research is necessary, corroborating the potential application of these in diagnosis and treatment of the disease.

Acknowledgements

Angel Juarez-Flores is a doctoral student from Programa de Posgrado en Ciencias Biológicas, Universidad Nacional Autónoma de México (UNAM), and a fellowship recipient from Consejo Nacional de Ciencia y Tecnología (CONACYT) (number: 775924). This paper constitutes a partial fulfilment of the Graduate Program in Biological Sciences of the UNAM. MVJ was financially supported by DGAPA PAPIIT-IN-224015, UNAM, México. We would like to thank Martha Cariño Aguilar for bibliographical support.

Disclosure of conflict of interest

None.

Address correspondence to: Marco V José, Theoretical Biology Group, Instituto de Investigaciones Biomédicas, Universidad Nacional Autónoma de México, CP 04510, Mexico City, Mexico. E-mail: marcojose@biomedicas.unam.mx

References

[1] Bray F, Ferlay J, Soerjomataram I, Siegel RL, Torre LA and Jemal A. Global cancer statistics 2018: GLOBOCAN estimates of incidence and mortality worldwide for 36 cancers in 185 countries. CA Cancer J Clin 2018; 68: 394-424.

[2] Siegel RL, Miller KD and Jemal A. Cancer statistics, 2018. CA Cancer J Clin 2018; 68: 7-30.

[3] Gridelli C, Rossi A, Carbone DP, Guarize J, Karachaliou N, Mok T, Petrella F, Spaggiari L and Rosell R. Non-small-cell lung cancer. Nat Rev Dis Primers 2015; 1: 15009.

[4] Inamura K. Lung cancer: understanding its molecular pathology and the 2015 WHO classification. Front Oncol 2017; 7: 193.

[5] Gandara DR, Hammerman PS, Sos ML, Lara PN Jr and Hirsch FR. Squamous cell lung cancer: from tumor genomics to cancer therapeutics. Clin Cancer Res 2015; 21: 2236-2243.

[6] Drilon A, Rekhtman N, Ladanyi M and Paik P. Squamous-cell carcinomas of the lung: emerging biology, controversies, and the promise of targeted therapy. Lancet Oncol 2012; 13: e418-426.

[7] Herbst RS, Morgensztern D and Boshoff C. The biology and management of non-small cell lung cancer. Nature 2018; 553: 446-454.

[8] Hirsch FR, Scagliotti GV, Mulshine JL, Kwon R, Curran WJ Jr, Wu YL and Paz-Ares L. Lung cancer: current therapies and new targeted treatments. Lancet 2017; 389: 299-311.

[9] Travis WD, World Health Organization. International agency for research on cancer, international academy of pathology. And international association for the study of lung cancer. Pathology and genetics of tumours of the lung, pleura, thymus and heart. Lyon: IARC Press, 2004.

[10] Davis S and Meltzer PS. GEOquery: a bridge between the gene expression omnibus (GEO) and bioconductor. Bioinformatics 2007; 23: 1846-1847.

[11] Ritchie ME, Phipson B, Wu D, Hu Y, Law CW, Shi W and Smyth GK. Limma powers differential expression analyses for RNA-sequencing and microarray studies. Nucleic Acids Res 2015; 43: e47.

[12] Schurch NJ, Schofield P, Gierlinski M, Cole C, Sherstnev A, Singh V, Wrobel N, Gharbi K, Simpson GG, Owen-Hughes T, Blaxter M and Barton GJ. How many biological replicates are needed in an RNA-seq experiment and which differential expression tool should you use? RNA 2016; 22: 839-851.

[13] Benjamini Y and Hochberg Y. Controlling the false discovery rate: a practical and powerful approach to multiple testing. Journal of the

Royal Statistical Society. Series B (Methodological) 1995; 57: 289-300.
[14] Glass K and Girvan M. Annotation enrichment analysis: an alternative method for evaluating the functional properties of gene sets. Sci Rep 2014; 4: 4191.
[15] Ackermann M and Strimmer K. A general modular framework for gene set enrichment analysis. BMC Bioinformatics 2009; 10: 47.
[16] Thomas PD, Campbell MJ, Kejariwal A, Mi H, Karlak B, Daverman R, Diemer K, Muruganujan A and Narechania A. PANTHER: a library of protein families and subfamilies indexed by function. Genome Res 2003; 13: 2129-2141.
[17] Calderone A, Castagnoli L and Cesareni G. Mentha: a resource for browsing integrated protein-interaction networks. Nat Methods 2013; 10: 690-691.
[18] Shannon P, Markiel A, Ozier O, Baliga NS, Wang JT, Ramage D, Amin N, Schwikowski B and Ideker T. Cytoscape: a software environment for integrated models of biomolecular interaction networks. Genome Res 2003; 13: 2498-2504.
[19] Assenov Y, Ramirez F, Schelhorn SE, Lengauer T and Albrecht M. Computing topological parameters of biological networks. Bioinformatics 2008; 24: 282-284.
[20] Dehmer M. Structural analysis of complex networks. Dordrecht; New York: Birkhäuser; 2011.
[21] Michibata H, Okuno T, Konishi N, Kyono K, Wakimoto K, Aoki K, Kondo Y, Takata K, Kitamura Y and Taniguchi T. Human GPM6A is associated with differentiation and neuronal migration of neurons derived from human embryonic stem cells. Stem Cells Dev 2009; 18: 629-639.
[22] Li S, Nikulina K, DeVoss J, Wu AJ, Strauss EC, Anderson MS and McNamara NA. Small proline-rich protein 1B (SPRR1B) is a biomarker for squamous metaplasia in dry eye disease. Invest Ophthalmol Vis Sci 2008; 49: 34-41.
[23] Michifuri Y, Hirohashi Y, Torigoe T, Miyazaki A, Fujino J, Tamura Y, Tsukahara T, Kanaseki T, Kobayashi J, Sasaki T, Takahashi A, Nakamori K, Yamaguchi A, Hiratsuka H and Sato N. Small proline-rich protein-1B is overexpressed in human oral squamous cell cancer stem-like cells and is related to their growth through activation of MAP kinase signal. Biochem Biophys Res Commun 2013; 439: 96-102.
[24] An G, Tesfaigzi J, Chuu YJ and Wu R. Isolation and characterization of the human spr1 gene and its regulation of expression by phorbol ester and cyclic AMP. J Biol Chem 1993; 268: 10977-10982.
[25] Candi E, Tarcsa E, Idler WW, Kartasova T, Marekov LN and Steinert PM. Transglutaminase cross-linking properties of the small proline-rich 1 family of cornified cell envelope proteins. Integration with loricrin. J Biol Chem 1999; 274: 7226-7237.
[26] Ly D, Zhu CQ, Cabanero M, Tsao MS and Zhang L. Role for high-affinity IgE receptor in prognosis of lung adenocarcinoma patients. Cancer Immunol Res 2017; 5: 821-829.
[27] Ra C, Nunomura S and Okayama Y. Fine-tuning of mast cell activation by fcepsilonribeta chain. Front Immunol 2012; 3: 112.
[28] Kuster H, Zhang L, Brini AT, MacGlashan DW and Kinet JP. The gene and cDNA for the human high affinity immunoglobulin E receptor beta chain and expression of the complete human receptor. J Biol Chem 1992; 267: 12782-12787.
[29] Gruber AD and Pauli BU. Molecular cloning and biochemical characterization of a truncated, secreted member of the human family of Ca2+-activated Cl- channels. Biochim Biophys Acta 1999; 1444: 418-423.
[30] Joosse SA, Hannemann J, Spotter J, Bauche A, Andreas A, Muller V and Pantel K. Changes in keratin expression during metastatic progression of breast cancer: impact on the detection of circulating tumor cells. Clin Cancer Res 2012; 18: 993-1003.
[31] Khanom R, Nguyen CT, Kayamori K, Zhao X, Morita K, Miki Y, Katsube K, Yamaguchi A and Sakamoto K. Keratin 17 Is induced in oral cancer and facilitates tumor growth. PLoS One 2016; 11: e0161163.
[32] Lessard JC, Pina-Paz S, Rotty JD, Hickerson RP, Kaspar RL, Balmain A and Coulombe PA. Keratin 16 regulates innate immunity in response to epidermal barrier breach. Proc Natl Acad Sci U S A 2013; 110: 19537-19542.
[33] Su W, Wang Y, Jia X, Wu W, Li L, Tian X, Li S, Wang C, Xu H, Cao J, Han Q, Xu S, Chen Y, Zhong Y, Zhang X, Liu P, Gustafsson JA and Guan Y. Comparative proteomic study reveals 17beta-HSD13 as a pathogenic protein in nonalcoholic fatty liver disease. Proc Natl Acad Sci U S A 2014; 111: 11437-11442.
[34] Chen J, Zhuo JY, Yang F, Liu ZK, Zhou L, Xie HY, Xu X and Zheng SS. 17-beta-hydroxysteroid dehydrogenase 13 inhibits the progression and recurrence of hepatocellular carcinoma. Hepatobiliary Pancreat Dis Int 2018; 17: 220-226.
[35] Hu J, Zhang LC, Song X, Lu JR and Jin Z. KRT6 interacting with notch1 contributes to progression of renal cell carcinoma, and aliskiren inhibits renal carcinoma cell lines proliferation in vitro. Int J Clin Exp Pathol 2015; 8: 9182-9188.
[36] Takahashi K, Paladini RD and Coulombe PA. Cloning and characterization of multiple hu-

man genes and cDNAs encoding highly related type II keratin 6 isoforms. J Biol Chem 1995; 270: 18581-18592.
[37] Katoh M and Katoh M. Identification and characterization of ASXL3 gene in silico. Int J Oncol 2004; 24: 1617-1622.
[38] Shukla V, Rao M, Zhang H, Beers J, Wangsa D, Wangsa D, Buishand FO, Wang Y, Yu Z, Stevenson HS, Reardon ES, McLoughlin KC, Kaufman AS, Payabyab EC, Hong JA, Zhang M, Davis S, Edelman D, Chen G, Miettinen MM, Restifo NP, Ried T, Meltzer PA and Schrump DS. ASXL3 is a novel pluripotency factor in human respiratory epithelial cells and a potential therapeutic target in small cell lung cancer. Cancer Res 2017; 77: 6267-6281.
[39] Johnson GS, Li J, Beaver LM, Dashwood WM, Sun D, Rajendran P, Williams DE, Ho E and Dashwood RH. A functional pseudogene, NMRAL2P, is regulated by Nrf2 and serves as a coactivator of NQO1 in sulforaphane-treated colon cancer cells. Mol Nutr Food Res 2017; 61.
[40] Yang S, He P, Wang J, Schetter A, Tang W, Funamizu N, Yanaga K, Uwagawa T, Satoskar AR, Gaedcke J, Bernhardt M, Ghadimi BM, Gaida MM, Bergmann F, Werner J, Ried T, Hanna N, Alexander HR and Hussain SP. A novel mif signaling pathway drives the malignant character of pancreatic cancer by targeting NR3C2. Cancer Res 2016; 76: 3838-3850.
[41] Arriza JL, Weinberger C, Cerelli G, Glaser TM, Handelin BL, Housman DE and Evans RM. Cloning of human mineralocorticoid receptor complementary DNA: structural and functional kinship with the glucocorticoid receptor. Science 1987; 237: 268-275.
[42] MacMillan-Crow LA and Thompson JA. Tyrosine modifications and inactivation of active site manganese superoxide dismutase mutant (Y34F) by peroxynitrite. Arch Biochem Biophys 1999; 366: 82-88.
[43] Kim YS, Gupta Vallur P, Phaeton R, Mythreye K and Hempel N. Insights into the dichotomous regulation of SOD2 in cancer. Antioxidants (Basel) 2017; 6.
[44] Shi Y, Xu X, Zhang Q, Fu G, Mo Z, Wang GS, Kishi S and Yang XL. tRNA synthetase counteracts c-Myc to develop functional vasculature. Elife 2014; 3: e02349.
[45] Lian Y, Niu X, Cai H, Yang X, Ma H, Ma S, Zhang Y and Chen Y. Clinicopathological significance of c-MYC in esophageal squamous cell carcinoma. Tumour Biol 2017; 39: 1010428-317715804.
[46] Todorov IT, Pepperkok R, Philipova RN, Kearsey SE, Ansorge W and Werner D. A human nuclear protein with sequence homology to a family of early S phase proteins is required for entry into S phase and for cell division. J Cell Sci 1994; 107: 253-265.
[47] Katayama H, Zhou H, Li Q, Tatsuka M and Sen S. Interaction and feedback regulation between STK15/BTAK/Aurora-A kinase and protein phosphatase 1 through mitotic cell division cycle. J Biol Chem 2001; 276: 46219-46224.
[48] Cheung CHY, Hsu CL, Chen KP, Chong ST, Wu CH, Huang HC and Juan HF. MCM2-regulated functional networks in lung cancer by multi-dimensional proteomic approach. Sci Rep 2017; 7: 13302.
[49] Tanaka H, Nakashiro K, Iwamoto K, Tokuzen N, Fujita Y, Shirakawa R, Oka R, Goda H and Hamakawa H. Targeting Aurora kinase A suppresses the growth of human oral squamous cell carcinoma cells in vitro and in vivo. Oral Oncol 2013; 49: 551-559.
[50] Singer JD, Gurian-West M, Clurman B and Roberts JM. Cullin-3 targets cyclin E for ubiquitination and controls S phase in mammalian cells. Genes Dev 1999; 13: 2375-2387.
[51] Loignon M, Miao W, Hu L, Bier A, Bismar TA, Scrivens PJ, Mann K, Basik M, Bouchard A, Fiset PO, Batist Z and Batist G. Cul3 overexpression depletes Nrf2 in breast cancer and is associated with sensitivity to carcinogens, to oxidative stress, and to chemotherapy. Mol Cancer Ther 2009; 8: 2432-2440.
[52] Miyazaki M and Esser KA. REDD2 is enriched in skeletal muscle and inhibits mTOR signaling in response to leucine and stretch. Am J Physiol Cell Physiol 2009; 296: C583-592.
[53] Morquette B, Morquette P, Agostinone J, Feinstein E, McKinney RA, Kolta A and Di Polo A. REDD2-mediated inhibition of mTOR promotes dendrite retraction induced by axonal injury. Cell Death Differ 2015; 22: 612-625.
[54] Zhang X, Luo F, Li J, Wan J, Zhang L, Li H, Chen A, Chen J, Cai T, He X, Lisse TS and Zhao H. DNA Damage-Inducible Transcript 4 is an innate guardian for human squamous cell carcinoma and an molecular vector for anti-carcinoma effect of 1,25(OH)2 D3. Exp Dermatol 2019; 28: 45-52.
[55] Eckhart L, Lippens S, Tschachler E and Declercq W. Cell death by cornification. Biochim Biophys Acta 2013; 1833: 3471-3480.

Table S1. List of differentially expressed genes in each stage

Metaplasia	FDR value	Mild dysplasia	FDR value	Moderate dysplasia	FDR value	Severe dysplasia	FDR value	carcinoma in situ	FDR value	squamous cell carcinoma of the lung	FDR value
ABCA12	0.011869	A2M	0.004649	ABCA12	0.000323	AADACL2	0.02205	AADACL2	3.42E-05	A2M	3.42E-06
ADAM22	0.003905	ABCA12	0.007564	ABI3BP	0.013267	ABCA12	0.002454	ABCA12	2.70E-05	AADAC	0.001164
ADGRF1	0.007158	ABI3BP	0.00166	ACTA2	0.015805	ABCA6	0.000223	ABCA6	0.000503	AADACL2	0.002055
AIM1L	0.013239	ACTA2	0.023463	ACTG2	0.01532	ABI3BP	0.003991	ABCC5	1.21E-07	ABCA1	8.66E-06
AKR1B1	0.007756	ACTG2	0.039314	ACTN2	0.006272	ACPP	0.000374	ABI3BP	0.005559	ABCA10	6.13E-06
AKR1B10	0.00148	ACTN2	0.025027	ADAMDEC1	0.0329	ACTG2	0.014572	ACTA2	0.001245	ABCA12	1.63E-07
AKR1C1	0.007756	ADAMTS9-AS2	0.00338	ADGRF1	0.001014	ACTN2	0.001164	ACTBL2	0.008969	ABCA13	4.75E-05
ALOX15B	0.008428	ADGRA2	0.005076	ADGRF4	0.000276	ADAM12	3.09E-05	ACTG2	0.004078	ABCA6	1.47E-08
ANKRD22	0.00277	ADGRF1	0.003616	AGBL2	0.033085	ADAM23	0.000783	ACTN2	0.002393	ABCA8	3.25E-07
ANLN	0.010235	ADGRF4	0.005379	AIM1L	1.36E-06	ADAMDEC1	0.000894	ACVR1C	6.62E-05	ABCC1	3.21E-07
ANXA10	0.040457	AIM1L	0.005401	AKR1B1	0.002084	ADAMTS9-AS2	0.000425	ADA	6.16E-06	ABCC5	8.68E-07
ARL14	0.030556	AKR1B10	0.002128	AKR1B10	3.84E-05	ADGRV1	0.000886	ADAM12	1.10E-07	ABCC6	8.98E-06
ASB5	0.025537	ALDH3A1	0.016178	ALDH4A1	0.000448	ADM	2.59E-05	ADAM23	1.73E-07	ABI3BP	1.42E-08
ASPM	0.011178	ALOX12	0.007057	ALOX12	0.013026	AFAP1-AS1	0.001411	ADAMDEC1	0.000462	ACOX2	2.00E-10
ATP13A5	0.038411	ANGPT1	0.002059	ALOX15B	0.00056	AHRR	0.005313	ADAMTS9-AS2	4.82E-05	ACP5	4.43E-08
AUNIP	0.025782	ANKRD22	0.001344	ANGPTL4	0.004788	AIM1L	0.002989	ADGRB3	0.000284	ACSS3	1.02E-08
AURKB	0.030719	ANLN	0.012932	ANKRD22	1.92E-06	AKR1B10	0.000208	ADGRF4	0.001376	ACTA2	0.000213
B3GNT6	0.033088	ANXA10	0.007475	ANLN	1.71E-05	AKR1C1	0.011953	ADGRV1	0.000546	ACTBL2	0.002526
BIRC5	0.006311	ANXA9	0.023455	ANXA10	0.014413	ALB	0.004592	ADM	4.89E-08	ACTG2	1.62E-05
BMP7	0.037062	APOBEC3A	0.036438	ANXA8L1	0.000692	ALPK2	0.00522	AFAP1-AS1	4.85E-06	ACTN2	4.29E-08
BRINP3	0.043771	APOBEC3B	0.002128	APOBEC3A	0.000118	ANGPTL1	0.001448	AHSG	0.0001	ACVR1C	2.91E-07
C12orf54	0.018301	ARHGAP11A	0.005929	APOBEC3B	1.33E-06	ANGPTL4	0.001573	AIM1L	0.000149	ADA	5.20E-10
C15orf48	0.027551	ARHGEF25	0.005366	AREG	0.000162	ANGPTL5	0.000997	AIM2	0.001452	ADAM12	2.88E-11
C3orf70	0.019854	ARL14	0.010677	ARHGAP11A	0.00011	ANKFN1	0.024549	AKAP12	4.87E-05	ADAM22	9.75E-07
CA12	0.020489	ASPG	0.005284	ARHGEF39	0.001643	ANKRD22	2.45E-05	AKR1B1	2.12E-06	ADAM23	5.00E-08
CALML5	0.017405	ASPM	0.009973	ARL14	0.000818	ANLN	8.04E-05	AKR1B10	2.74E-07	ADAMDEC1	4.65E-06
CAPN14	0.025881	ASPN	0.002977	ARMC3	0.041788	ANXA10	0.036585	AKR1C1	5.12E-07	ADAMTS4	1.83E-07
CAPN6	0.018936	ATP13A5	0.007354	ARNTL2	3.02E-06	APOBEC3A	0.001916	AKR1C3	9.30E-06	ADAMTS8	2.22E-06
CASQ2	0.006311	ATP1A2	0.011702	ASB5	0.01354	APOBEC3B	3.90E-06	ALOX12	0.000317	ADAMTS9-AS2	4.80E-10
CCK	0.013228	ATP1B2	0.002059	ASF1B	1.60E-05	APOBEC3D	0.000105	AMPD1	0.004121	ADAMTSL3	7.91E-10
CDCA2	0.009764	AUNIP	0.009692	ASPA	0.004577	AREG	0.000109	ANGPTL1	5.85E-05	ADARB2	1.68E-05
CDKN3	0.00277	AURKB	0.005275	ASPG	0.001697	ARHGAP11A	2.34E-06	ANGPTL4	0.000664	ADCY10	6.30E-06
CEACAM5	0.010235	B3GNT6	0.028688	ASPM	2.35E-05	ARHGAP8	0.000806	ANGPTL5	0.002427	ADCY2	1.44E-10
CEMIP	0.010139	BHLHE22	0.026907	ASPN	0.021227	ARHGEF39	0.002444	ANGPTL7	0.023857	ADCY7	7.23E-11
CENPA	0.028401	BHMT2	0.009276	ATP1A2	0.022122	ARNTL2	2.10E-06	ANKRD22	1.12E-05	ADGB	3.53E-05
CEP55	0.002809	BIRC5	0.003616	AUNIP	0.000224	ASF1B	3.28E-05	ANLN	0.000223	ADGRB3	1.86E-07
CKAP2L	0.040631	BMP7	0.018907	AURKA	1.51E-05	ASPM	2.43E-05	ANOS1	2.22E-07	ADGRE1	1.91E-06

CLCA3P	0.00277	BNC2	0.005401	AURKB	0.000235	ASXL3	0.000187	ANXA10	0.025363	ADGRF4	3.22E-06
CLCA4	0.046515	C1orf186	0.003254	BCHE	0.029054	ATAD2	5.21E-06	ANXA9	0.007441	ADGRG2	4.60E-06
CNTN4	0.013228	C1QTNF7	0.005973	BHMT2	0.003965	ATP1A2	0.002239	APOBEC3A	0.001174	ADGRV1	3.09E-05
CPA4	0.01576	C1S	0.010682	BICD2	0.000531	ATP1B3	8.98E-05	APOBEC3B	3.98E-08	ADH1A	2.48E-12
CPED1	0.030556	CA6	0.040427	BIRC5	1.39E-06	AUNIP	9.56E-05	APOBEC3D	2.41E-06	ADH1C	2.18E-11
CREG2	0.036408	CALD1	0.003789	BMP7	0.000197	AURKA	4.72E-06	AR	1.50E-06	ADH6	0.001464
CSTA	0.00148	CALML5	0.007959	BNC1	0.004712	AURKB	0.000331	AREG	0.000379	ADIRF	5.71E-11
CYP3A4	0.00706	CAPN14	0.001797	BRINP3	0.004862	BCL2A1	0.003119	ARHGAP11A	5.84E-05	ADM	1.03E-12
CYP3A5	0.007756	CAPN6	0.010571	BUB1	0.000162	BIRC5	6.96E-07	ARHGAP6	2.07E-05	ADRA1B	2.11E-05
CYP3A7	0.007756	CCDC102B	0.009276	BUB1B	6.36E-05	BMP7	0.001747	ARHGEF39	0.000434	ADRA2A	3.57E-09
DEPDC1B	0.007756	CCK	0.005378	C10orf82	0.011369	BNC1	0.002203	ARL14	0.000962	ADTRP	2.30E-05
DKK1	0.006896	CCL19	0.034532	C11orf88	0.03544	BNC2	0.003145	ARNTL2	6.91E-07	AFAP1-AS1	8.00E-07
DLGAP5	0.005268	CCNA2	0.002128	C12orf54	0.001234	BRIP1	0.000201	ASF1B	2.80E-06	AGBL2	3.54E-05
DOCK3	0.018512	CDC25C	0.014608	C15orf48	5.56E-05	BUB1	1.46E-05	ASPA	0.000145	AGR2	2.99E-07
DSG3	0.009515	CDCA2	0.004453	C1orf186	0.005575	BUB1B	1.82E-05	ASPM	1.33E-06	AGR3	3.12E-07
EGFEM1P	0.040519	CDH16	0.010794	C20orf85	0.035913	C12orf54	0.001367	ASXL3	1.87E-07	AIM1L	7.31E-06
EPHA3	0.036763	CDKN3	0.003156	C3orf70	0.011848	C14orf37	1.97E-05	ATAD2	1.73E-07	AIM2	7.99E-08
ERCC6L	0.042429	CDO1	0.013187	C8orf34	0.001587	C15orf48	0.000594	ATP13A5	0.015684	AJAP1	3.77E-05
ESCO2	0.009491	CENPA	0.015642	C9orf135	0.045469	C16orf59	2.87E-06	ATP1A2	0.000281	AK7	7.23E-05
FABP5	0.00704	CENPM	0.004606	C9orf24	0.031503	C17orf53	0.000147	ATP1B3	9.89E-08	AK8	5.53E-05
FAM83A	0.017003	CENPN	0.002435	CA12	0.000218	C1QTNF7	0.004854	ATP8B3	0.000269	AK9	2.86E-07
FETUB	0.00706	CEP55	0.005929	CACNG6	0.006314	C6orf10	0.000359	AUNIP	1.14E-05	AKAP12	9.18E-10
FGFBP1	0.004933	CLCA3P	0.001313	CALML5	0.000421	C6orf118	0.017753	AURKA	5.79E-06	AKAP14	2.40E-06
GABRG1	0.014892	CLCA4	0.030489	CAPN14	7.75E-05	C6orf15	0.017753	AURKB	4.77E-05	AKAP6	2.41E-06
GATA5	0.031462	CLDN17	0.031912	CAPN6	0.033714	C8orf34	0.000204	BCL2A1	0.001328	AKR1B1	1.95E-07
GDPD2	0.049611	CNN1	0.048166	CAPS2	0.011336	C9orf47	0.000584	BICD2	0.00057	AKR1B10	2.98E-05
GPM6A	0.006311	CNRIP1	0.001906	CAPSL	0.038175	CA12	0.00185	BIRC5	5.36E-08	AKR1C1	6.34E-06
GPX2	0.006747	COL14A1	0.001553	CARD14	0.000124	CACNB2	0.002115	BLACAT1	0.00168	ALB	0.000476
GRHL3	0.005758	COL1A2	0.01079	CASQ2	0.00115	CACNB4	0.001084	BMP7	0.001455	ALDH18A1	0.000455
GTSE1	0.021846	COL3A1	0.012672	CATSPERD	0.018308	CALML5	0.003013	BNC1	0.000274	ALDH1A1	1.57E-09
HIST1H1B	0.036469	COL4A4	0.005825	CCK	0.002184	CAPN14	0.009438	BNC2	0.000533	ALDH1L1	4.30E-08
HMMR	0.006928	COL6A1	0.005929	CCNA2	7.08E-06	CAPN6	0.007594	BRIP1	0.000323	ALDH3B1	4.49E-09
HTR3A	0.040735	COL6A6	0.015404	CCNB1	2.17E-05	CAPS2	0.003771	BUB1	3.90E-05	ALDH7A1	1.83E-14
IL1RN	0.00148	COL8A1	0.011866	CCNB2	8.55E-06	CARD14	3.57E-05	BUB1B	1.40E-05	ALOX12	0.007643
IL36G	0.036632	CPA3	0.001344	CD109	3.83E-06	CARD18	0.003863	C10orf82	0.002341	ALOX15	4.44E-08
INSL4	0.042901	CPA4	0.003096	CDC20	0.000146	CASC9	0.015132	C12orf54	0.00053	ALPK2	1.13E-07
IVL	0.016544	CPED1	0.004443	CDC25C	0.000922	CASQ2	0.005349	C14orf37	0.000444	ALS2CR12	0.000122
KCNA5	0.036827	CREG2	0.033228	CDC45	2.83E-06	CCDC150	0.000243	C15orf48	0.000494	AMH	7.72E-07
KCNJ1	0.013691	CRNN	0.018752	CDC6	0.000144	CCDC38	0.002742	C16orf59	1.56E-08	AMPD1	0.000875
KIAA1644	0.030913	CSTA	0.001344	CDCA2	7.08E-06	CCK	0.020611	C17orf53	4.39E-05	AMY1C	7.19E-07
KLK7	0.009012	CTSG	0.015109	CDCA3	7.25E-06	CCL18	0.024621	C1QTNF2	0.000142	ANG	5.08E-09

KLK8	0.001726	CTSK	0.004413	CDCA5	6.31E-06	CCL20	0.005327	C1QTNF7	6.54E-05	ANGPTL1	4.16E-12
KRT13	0.04607	CXCL12	0.004535	CDCA8	8.96E-06	CCNA2	8.99E-06	C3orf70	0.004065	ANGPTL4	1.59E-08
KRT16	0.001873	CYP3A4	0.002133	CDH16	0.000252	CCNB1	8.93E-06	C4BPA	0.027644	ANGPTL5	1.28E-07
KRT16P3	0.007756	CYP3A5	0.003904	CDK1	3.71E-05	CCNB2	1.26E-06	C6orf10	0.0003	ANGPTL7	0.000127
KRT6B	0.010846	CYP3A7	0.00338	CDKN3	1.75E-06	CCNYL1	1.16E-07	C6orf15	0.002427	ANKFN1	0.001791
KRT6C	0.00092	DACH1	0.008706	CEACAM5	0.004309	CD109	0.000178	C7	0.012045	ANKRD22	5.98E-07
LINC01589	0.007756	DACT1	0.018391	CEMIP	0.001576	CDC20	0.000254	C8orf88	5.26E-06	ANKRD42	5.73E-06
LYPD3	0.001885	DACT3	0.002357	CENPA	4.76E-06	CDC25C	0.000265	CA12	0.000591	ANKRD66	1.85E-05
MCM10	0.016873	DCN	0.001797	CENPE	3.82E-05	CDC45	5.86E-07	CACNB2	0.001611	ANKUB1	0.000132
MELK	0.008177	DDX3Y	0.041951	CENPF	6.82E-05	CDC6	9.06E-07	CALB1	0.005881	ANLN	1.71E-08
NCAPG	0.006228	DEPDC1B	0.008014	CENPK	0.000399	CDCA2	2.18E-06	CALB2	0.008543	ANOS1	7.70E-14
NMRAL1P1	0.009871	DES	0.04743	CENPM	5.56E-05	CDCA3	1.82E-06	CALML5	0.00349	ANXA10	3.44E-05
NMU	0.006311	DKK1	0.001945	CENPN	9.33E-06	CDCA5	5.86E-07	CAPN14	0.008852	ANXA8L1	0.000227
NPAS3	0.008862	DLGAP5	0.004342	CENPW	4.67E-07	CDCA7	0.000336	CAPN6	0.001544	AOC3	3.90E-05
PBK	0.007166	DNM3OS	0.009653	CEP55	1.79E-06	CDCA8	8.17E-06	CARD14	1.50E-06	AOX1	0.000527
PHLDA2	0.006268	DOK6	0.003904	CERS3	0.030514	CDH16	0.021714	CARD18	0.000732	AP5B1	4.19E-05
PLN	0.021479	DPT	0.002537	CFAP43	0.048658	CDH24	0.001046	CASC9	4.48E-07	APBA2	3.36E-10
PPP2R2C	0.042312	DSG3	0.008937	CFAP54	0.009534	CDK1	2.00E-05	CASQ2	0.001042	APCDD1L	9.22E-06
PRSS2	0.00277	EBF1	0.003124	CHEK1	1.14E-05	CDKN2A	0.001888	CBLN2	0.021411	APLN	4.06E-07
PRSS3	0.00148	EBF3	0.004291	CKAP2L	0.000421	CDKN3	6.86E-06	CCDC150	4.03E-05	APOBEC2	1.92E-06
PTPRH	0.010235	ECM2	0.001553	CKS2	3.90E-05	CDO1	0.040611	CCDC177	1.43E-05	APOBEC3A	1.03E-05
PTTG3P	0.015339	EGFEM1P	0.036102	CLCA3P	1.14E-06	CDSN	0.003064	CCDC38	0.000455	APOBEC3B	2.14E-08
RERGL	0.024062	EIF1AY	0.021813	CLCA4	0.000101	CDT1	6.53E-05	CCL20	3.35E-05	APOC1	9.98E-07
RGS20	0.007166	ELN	0.020133	CLDN17	0.016647	CENPA	3.98E-05	CCL23	0.003163	APOC2	0.000463
RRM2	0.006268	EMCN	0.007152	CNN1	0.014932	CENPE	1.62E-05	CCNA2	2.04E-05	APOD	9.41E-05
RTKN2	0.001726	EPGN	0.010682	COL14A1	0.005687	CENPF	1.53E-05	CCNB2	2.83E-07	APOE	0.000168
S100A2	0.010839	EPHA3	0.004291	CPA3	0.009292	CENPK	0.00058	CCNE1	8.68E-08	APOL1	3.62E-07
S100A7	0.004933	ERCC6L	0.005752	CPA4	0.000253	CENPL	2.05E-05	CD1A	0.007027	AQP3	1.52E-06
S100A8	0.002809	EREG	0.005197	CPED1	0.001437	CENPM	1.23E-05	CD274	0.001479	AQP5	4.47E-11
S100A9	0.001726	ESCO2	0.006074	CRB1	0.00191	CENPN	1.47E-06	CDC25C	0.000169	AQP6	6.53E-08
SBSPON	0.039491	F2RL2	0.016011	CREG2	0.001437	CENPP	1.27E-05	CDC45	3.80E-09	AQP9	0.0009
SCEL	0.001726	FABP5	0.003616	CRMP1	0.004788	CENPU	5.30E-05	CDC6	4.24E-07	AR	3.07E-13
SEC14L3	0.043591	FAM19A2	0.001752	CRNN	0.008759	CENPW	2.15E-05	CDCA2	8.14E-07	ARFGEF3	4.54E-09
SERPINB13	0.021479	FAM83A	0.006032	CSTA	1.33E-06	CEP55	1.39E-06	CDCA3	5.18E-07	ARG1	0.001111
SERPINB2	0.011869	FAM83C	0.011307	CTSV	0.000203	CERS3	0.00731	CDCA5	5.43E-09	ARHGAP11A	3.38E-09
SERPINB5	0.002641	FAP	0.008221	CTXN2	0.004544	CFAP47	0.013851	CDCA7	4.79E-06	ARHGAP20	1.35E-11
SH2D1B	0.009936	FBLN1	0.002435	CYP3A4	0.002228	CFAP54	0.003905	CDCA8	1.63E-06	ARHGAP30	4.80E-07
SLC13A5	0.03517	FBN1	0.004703	CYP3A5	8.12E-05	CFAP70	0.015247	CDH16	0.004223	ARHGAP44	9.56E-07
SLC16A12	0.012533	FETUB	0.003616	CYP3A7	1.50E-05	CHEK1	2.87E-06	CDH19	0.007361	ARHGAP6	4.47E-10
SLC7A11	0.005073	FGF7	0.001797	DACT3	0.006753	CHRNA3	0.001946	CDH24	6.50E-05	ARHGAP8	7.37E-05

SLITRK3	0.033857	FGFBP1	0.003616	DAW1	0.026389	CHRNA5	0.000682	CDHR1	0.001782	ARHGEF39	5.79E-08
SMOC2	0.013778	FLRT2	0.002059	DEFB103B	0.00556	CKAP2L	0.000355	CDK1	2.49E-06	ARL11	5.19E-10
SORBS1	0.036408	FOXF2	0.002722	DEFB4A	0.001678	CKS2	3.17E-05	CDKN2A	0.000821	ARL14	0.000361
SPC25	0.006747	FREM1	0.00338	DENND5B	0.000496	CLCA3P	0.009762	CDKN3	6.06E-06	ARMC2	1.10E-05
SPINK5	0.038143	FRZB	0.009228	DEPDC1	0.001507	CLEC4D	0.007566	CDO1	0.008218	ARMC3	6.57E-06
SPRR1A	0.006107	GALNT5	0.002128	DEPDC1B	9.12E-06	CLEC7A	0.002169	CDSN	0.000296	ARMC4	6.06E-06
SPRR1B	0.000812	GCNT3	0.032035	DES	0.009909	CLIP4	8.33E-05	CDT1	1.68E-06	ARNTL2	4.09E-11
SPRR2C	0.039804	GDF10	0.048443	DIAPH3	6.82E-05	CLSPN	0.001063	CECR2	5.62E-05	ART3	0.000136
SPRR2D	0.014608	GDPD2	0.004511	DKK1	3.53E-05	CNN1	0.008737	CENPA	1.69E-06	ASAP1	4.73E-09
SPRR3	0.004502	GEM	0.003018	DLGAP5	1.25E-05	CNTN3	0.000788	CENPE	2.81E-05	ASB14	0.001886
SYNE1	0.046445	GJB6	0.006023	DMD	0.011108	CNTN4	0.001417	CENPF	5.49E-07	ASB4	3.36E-06
SYNPO2	0.043756	GLT8D2	0.00546	DNAH12	0.045881	COCH	0.00018	CENPL	1.65E-05	ASB5	6.05E-05
TICRR	0.00706	GPM6A	0.001752	DNAH7	0.032644	COL21A1	0.003007	CENPM	3.44E-06	ASCL1	7.96E-08
TMEM108	0.015385	GPX2	0.005076	DOCK3	0.006231	COLEC11	0.000461	CENPN	2.05E-07	ASCL3	0.005868
TMPRSS11B	0.025537	GRHL3	0.007453	DSC2	2.95E-05	CPED1	0.006255	CENPP	1.73E-07	ASF1B	3.01E-09
TMPRSS11D	0.040735	GSDMC	0.010815	DSG3	9.14E-06	CRB1	0.001342	CENPU	5.66E-07	ASPA	5.83E-11
TMPRSS11E	0.031086	GTSE1	0.007475	DSP	0.002616	CRCT1	0.007821	CENPW	4.31E-05	ASPM	8.46E-11
TOP2A	0.024198	GUCY1A2	0.009629	DTL	0.000389	CREG2	0.014891	CEP55	1.65E-06	ASTN2	5.67E-07
TTK	0.007166	GZMK	0.007475	DUOX2	0.003395	CRNN	0.029729	CERS3	0.000433	ASXL3	1.70E-12
UBE2C	0.010139	HAPLN1	0.002818	DYDC1	0.046332	CSH1	0.000267	CFHR4	3.86E-07	ATAD2	2.05E-12
ULBP2	0.008177	HDC	0.004239	DYNLRB2	0.028214	CSTA	3.17E-05	CHEK1	9.63E-08	ATAD5	5.94E-09
UPK1B	0.034741	HJURP	0.019553	E2F1	1.06E-06	CTSV	0.001176	CHODL	0.000615	ATOH8	2.88E-13
ZBED2	0.002641	HOXA3	0.001344	E2F2	2.66E-06	CXCL13	0.003349	CHRNA3	0.000316	ATP12A	4.51E-06
		HOXA4	0.002128	ECT2L	0.037122	CYP1A1	0.010374	CKAP2L	5.50E-05	ATP1A2	6.75E-14
		HPGDS	0.001752	EFCAB1	0.023714	CYP27B1	3.43E-05	CKMT2	0.000255	ATP1B2	5.11E-06
		HSD17B13	0.038944	EGFEM1P	0.003994	CYP2A6	0.023214	CKS2	2.45E-05	ATP2C2	1.41E-07
		HSPB2	0.002128	EGR4	0.00563	CYP2A7	0.023542	CLCA3P	0.007118	ATP6V0D2	0.001575
		HTR2A	0.019584	ELOVL6	0.000227	CYP2F1	0.000726	CLDN17	0.008803	ATP6V1G3	0.000151
		HTRA3	0.001705	EMP1	9.30E-06	DACT3	0.008467	CLEC4D	0.003316	AUNIP	8.27E-11
		IGK	0.046997	EPHA3	0.008018	DCDC5	0.007137	CLEC7A	0.000234	AURKA	3.11E-10
		IGLC1	0.026638	EPHA5-AS1	0.004899	DDIAS	2.10E-06	CLIP4	1.57E-06	AURKB	1.27E-07
		IGLJ3	0.033472	ERCC6L	0.000144	DEFB103B	8.07E-05	CLSPN	0.003414	AVPR2	1.58E-08
		IGLL1	0.046779	EREG	0.007681	DEFB4A	8.86E-05	CNGB3	4.18E-06	AXIN2	1.26E-08
		IL1RN	0.001705	ERICH3	0.031091	DEPDC1	0.00222	CNN1	0.003992	AZGP1	0.018962
		IL36G	0.012228	ESCO2	5.42E-06	DEPDC1B	4.75E-05	CNTN2	0.02591	B3GNT4	2.93E-06
		INSL4	0.004994	ESPL1	2.86E-06	DES	0.006111	CNTN4	0.000352	B4GALNT1	2.12E-10
		ITGA7	0.003096	EXO1	0.000345	DHRS2	0.012916	CNTNAP2	0.000105	B4GALNT4	1.34E-07
		ITGA8	0.006994	FABP5	4.65E-06	DIAPH3	0.000321	COCH	9.17E-05	B9D1	1.27E-05
		ITGBL1	0.01953	FAM111B	0.000813	DKFZp547J222	0.000309	COL14A1	0.00988	BACH1	7.95E-10
		ITM2A	0.00245	FAM126A	0.00102	DKK1	0.000582	COLEC11	0.000215	BAIAP3	2.93E-05

IVL	0.004516	FAM132A	0.000287	DLGAP5	1.33E-05	COX7A1	0.000188	BARX1	4.73E-07
JAM2	0.005375	FAM20C	0.006191	DMD	0.002383	CPA6	7.25E-06	BBOF1	5.84E-05
JCHAIN	0.009144	FAM227B	0.008207	DNAH12	0.034848	CPED1	0.000526	BCAT1	2.08E-07
KCNJ8	0.005756	FAM72D	0.000236	DNAH5	0.003328	CRCT1	0.001381	BCHE	0.035833
KCNK10	0.016553	FAM83A	8.62E-05	DNAH7	0.029407	CRNN	0.00181	BCL2A1	1.51E-07
KCTD16	0.006707	FAM83C	0.005533	DPY19L2P2	0.022636	CSH1	0.000154	BEND7	2.65E-08
KIAA0101	0.002059	FAR1	0.000159	DSC2	8.51E-05	CSTA	2.89E-07	BEX1	4.11E-06
KIAA1755	0.003381	FAR2P2	0.006272	DSG3	2.98E-05	CTSV	4.79E-05	BHMT2	7.81E-05
KIF20A	0.008492	FETUB	5.42E-05	DSP	0.000556	CXCL12	0.019142	BICD2	7.87E-07
KLK13	0.004516	FGFBP1	2.35E-05	DTL	2.05E-05	CXCL13	0.000535	BID	1.99E-12
KLK7	0.013062	FILIP1	0.002138	DUOX2	0.003632	CXCL5	0.000807	BIRC5	2.88E-11
KLK8	0.01902	FLJ30901	0.011722	E2F1	1.75E-07	CYP2A13	0.000318	BIRC7	3.47E-05
KRT13	0.009486	FNDC1	0.032976	E2F2	6.11E-05	CYP2A6	0.013973	BLACAT1	0.000289
KRT16	0.001344	FOXM1	3.46E-05	ECT2	1.16E-07	CYP2A7	0.015879	BLM	6.63E-07
KRT16P3	0.00245	FRZB	0.043972	EDIL3	0.000763	CYP2F1	5.13E-05	BMP1	6.63E-07
KRT24	0.005825	FSCN1	0.000271	EDN2	0.002403	CYP4B1	0.001361	BMP3	1.87E-06
KRT4	0.011263	GAL	0.016648	EFHB	0.015948	CYP4F11	5.13E-05	BMP4	1.50E-08
KRT6B	0.003895	GALNT5	0.000297	EGFEM1P	0.001317	CYP4F3	0.004435	BMP5	0.001315
KRT6C	0.001737	GATA5	0.015937	EGR4	0.000404	DACT1	0.010966	BMP8B	8.96E-08
KRT77	0.012447	GCNT3	0.028588	EPHA3	0.009255	DACT3	0.00349	BMPR1B	2.93E-07
KRTDAP	0.039897	GDPD2	0.001016	ERBB4	0.007593	DAPL1	0.002983	BPIFB1	1.65E-06
LEPR	0.003616	GINS2	1.32E-05	ERCC6L	0.000132	DCN	0.00988	BRCA2	1.84E-08
LGALS1	0.002741	GJB2	0.004153	ERICH3	0.033946	DDIAS	1.42E-08	BRINP3	9.81E-06
LHFP	0.002059	GJB6	1.50E-05	ERVMER34-1	2.67E-05	DEFB103B	7.95E-06	BRIP1	1.26E-08
LINC00707	0.002059	GPM6A	2.56E-05	ESCO2	1.64E-05	DEFB126	1.48E-06	BTC	1.28E-10
LINC01197	0.009907	GPRC5D	0.008386	ESPL1	1.41E-05	DEFB4A	0.000243	BTG4	0.00037
LINC01559	0.003673	GPX2	0.002135	EXO1	3.48E-05	DEPDC1B	1.12E-05	BTNL9	2.16E-05
LINC01589	0.01854	GRHL3	1.51E-05	EZH2	4.06E-07	DES	0.002286	BUB1	7.83E-08
LRCH2	0.007387	GRID2	0.000783	FABP5	0.000237	DGAT2	9.82E-05	BUB1B	4.74E-10
LSAMP	0.006966	GSDMC	0.000565	FAM110C	2.87E-06	DIAPH3	3.35E-05	C10orf107	5.80E-06
LTBP1	0.00335	GSG2	5.29E-06	FAM111B	0.000193	DIO3OS	0.007844	C10orf111	1.61E-06
LUM	0.002383	GTSE1	1.29E-05	FAM13A	0.002596	DKK1	1.36E-05	C10orf67	0.000449
LY6D	0.037032	HAPLN1	0.031235	FAM20C	0.00668	DLG2	7.89E-05	C10orf82	1.62E-05
LYPD3	0.008821	HAS3	0.002515	FAM72D	0.00051	DLGAP5	3.12E-05	C11orf16	3.00E-06
MALL	0.011467	HIST1H1B	0.007167	FAM83A	0.005353	DMD	0.007116	C11orf52	9.86E-08
MCM10	0.013194	HIST1H3B	7.28E-05	FAM83C	0.019154	DMRTC1	3.08E-05	C11orf70	1.26E-05
MELK	0.006731	HJURP	0.00192	FANCI	5.44E-07	DNA2	3.06E-05	C11orf87	3.71E-05
MEOX2	0.004923	HKDC1	0.012152	FETUB	6.74E-05	DPT	0.001076	C11orf88	2.56E-06
MFAP4	0.003616	HMMR	7.25E-06	FGF14	0.015493	DQX1	4.92E-07	C14orf132	4.25E-09
MFAP5	0.040063	HOXA3	0.007394	FGFBP1	0.001736	DSC1	0.000622	C14orf37	4.69E-06

MGP	0.001752	HS6ST3	0.020598	FILIP1	0.000321	DSC2	1.69E-07	C15orf48	4.54E-05
MKI67	0.027616	HSD17B13	0.002105	FLJ30901	0.014781	DSC3	0.025836	C16orf59	4.86E-12
MMP16	0.008531	HSPB7	0.011336	FLRT3	0.001101	DSG3	2.13E-07	C16orf71	8.22E-06
MOXD1	0.008377	HTR3A	0.0007	FMN2	0.004992	DTL	1.11E-07	C16orf89	1.22E-09
MREG	0.002128	IL1RN	4.67E-07	FMO2	0.00053	DUOX2	0.000979	C17orf53	1.20E-10
MS4A2	0.001313	IL20RB	0.00339	FOXE1	0.001982	DUSP12	1.12E-05	C17orf97	7.46E-05
MXRA8	0.005676	IL36G	2.38E-06	FOXL2	5.91E-06	DUSP26	0.000679	C1orf101	6.09E-06
MYH11	0.030257	IL36RN	0.001573	FOXM1	4.51E-06	DUSP5P1	0.00298	C1orf158	8.38E-06
MYLK	0.005366	INSL4	0.002167	FPR2	0.011357	DYNC1I1	0.00116	C1orf168	9.20E-08
MYOC	0.015033	IQUB	0.038182	FRZB	0.034497	E2F1	5.69E-09	C1orf64	0.000284
NAP1L3	0.003877	IVL	9.25E-06	FSCN1	0.000925	ECE2	2.18E-08	C1orf87	2.22E-05
NAV3	0.019844	KCNA4	0.001295	GAL	1.15E-06	ECT2	3.43E-10	C1QA	1.37E-05
NCAPG	0.003498	KCNA5	0.029844	GAST	1.47E-06	EDIL3	0.0082	C1QC	3.78E-08
NDC80	0.012228	KCNK10	0.006007	GDA	0.006008	EDN2	0.000367	C1QTNF2	4.82E-08
NEGR1	0.007322	KCNMB2	0.020967	GDPD2	0.013767	EGR4	4.13E-06	C1QTNF4	7.42E-08
NEXN	0.023451	KCTD16	9.47E-05	GINS2	2.87E-06	EIF5A2	7.90E-06	C1QTNF7	3.44E-10
NMRAL1P1	0.006196	KHDRBS2	0.011313	GINS4	0.001451	ELN	0.013374	C20orf85	1.28E-05
NMU	0.002457	KIAA0101	7.72E-07	GJA3	0.02112	EPHA3	0.00196	C21orf58	0.000179
NUSAP1	0.006754	KIAA0408	0.003342	GJB6	0.000426	ERBB4	0.001725	C22orf15	5.94E-06
OGN	0.002128	KIAA1549L	0.021932	GLT1D1	0.000209	ERCC6L	6.39E-05	C22orf23	1.38E-05
OLFM4	0.023935	KIAA1644	0.008648	GNGT1	0.002815	ERVMER34-1	5.54E-07	C2orf40	1.22E-06
OMD	0.004738	KIF11	0.001474	GPM6A	4.18E-05	ESCO2	6.94E-07	C2orf70	0.000147
OSR2	0.00301	KIF15	3.56E-05	GPR158	0.004473	ESPL1	9.24E-07	C2orf73	5.25E-05
P2RY14	0.002059	KIF18A	0.001798	GPRC5D	0.004518	ETV1	0.000786	C4orf22	2.74E-05
PBK	0.00315	KIF20A	7.75E-05	GPX2	0.000974	ETV4	0.00063	C6	0.012495
PCDH18	0.002655	KIF23	1.29E-05	GREM1	0.026886	EXO1	3.77E-06	C6orf10	1.30E-06
PDE5A	0.005922	KIF2C	5.07E-05	GRHL3	0.000195	EZH2	3.80E-09	C6orf118	1.16E-05
PDGFRA	0.012161	KIF4A	0.000414	GRID2	0.00469	FABP4	0.011631	C6orf15	0.005353
PDGFRB	0.003124	KIFC1	0.000113	GRM5	0.002222	FABP5	1.25E-05	C6orf52	0.000125
PDLIM3	0.008377	KLHL32	0.003225	GRM7	0.004611	FAM107A	8.56E-05	C6orf58	0.002582
PDZRN3	0.002032	KLK13	0.015798	GSDMC	0.001554	FAM110C	9.89E-07	C7	3.64E-05
PDZRN4	0.017816	KLK7	1.22E-06	GSG2	3.14E-06	FAM111B	0.000669	C8orf34	0.000295
PGM5	0.001752	KLK8	4.59E-05	GSTM3	0.004377	FAM72D	1.09E-05	C8orf46	1.74E-07
PGR	0.003591	KRT13	3.84E-05	GTSE1	5.08E-06	FAM83A	0.00673	C8orf88	2.35E-06
PI16	0.001344	KRT14	0.008018	GZMB	0.004097	FAM83C	0.001602	C9orf116	3.47E-05
PLN	0.028418	KRT16	7.40E-08	HAPLN1	0.002951	FAM89A	7.95E-07	C9orf135	2.10E-05
PLPPR4	0.012539	KRT16P3	1.14E-06	HAS3	0.000239	FANCI	3.01E-07	C9orf24	9.44E-06
PNMAL1	0.002383	KRT24	2.21E-05	HHLA2	0.004954	FETUB	0.000661	C9orf66	2.44E-07
PNOC	0.047647	KRT34	0.019206	HIF3A	0.005915	FGF7	2.98E-05	CA10	0.000406
PPP2R2C	0.001852	KRT6B	4.81E-07	HIST1H1B	0.0108	FGFBP1	0.008652	CA3	1.12E-06

PRR16	0.014608	KRT6C	1.09E-07	HIST1H3B	7.22E-05	FHL1	0.002074	CA6	0.010077
PRSS2	0.001344	KRT79	0.002614	HIST1H3D	6.54E-05	FLG	6.25E-05	CA9	3.47E-05
PRSS27	0.010176	KRTDAP	0.026483	HJURP	0.000929	FLJ30901	0.011997	CAB39L	9.84E-13
PRSS3	0.002128	LAD1	4.15E-07	HMGA2	0.002527	FLRT3	0.002182	CACNB2	1.80E-06
PRUNE2	0.042241	LCE3A	0.003055	HMGCS1	0.000137	FMO2	0.000114	CACNB4	1.56E-09
PSCA	0.010115	LCE3D	0.032571	HMMR	6.09E-05	FNDC5	0.001568	CACNG6	9.19E-05
PTCHD1	0.029213	LGALS7	0.000715	HOXA10	0.000447	FOXE1	1.77E-05	CADM1	9.95E-06
PTGDS	0.007354	LGALS7B	0.000758	HOXA11-AS	0.010844	FOXL2	1.08E-08	CALB1	2.37E-06
PTGIS	0.04061	LINC00326	0.021315	HOXA9	0.001017	FOXM1	9.89E-07	CALB2	0.000316
PTPRH	0.012506	LINC00707	1.78E-05	HOXB13	0.038286	FPR2	0.016051	CALCA	1.02E-06
PTTG3P	0.006327	LINC00892	0.007372	HOXC13	0.000244	FRZB	0.014989	CALML4	2.00E-07
RCAN2	0.004443	LINC01559	0.009753	HOXC9	0.000241	FSCN1	2.18E-05	CAMP	0.016279
RECK	0.001724	LINC01589	0.012907	HOXD10	0.001518	FSTL4	0.004955	CAPN14	0.02176
RFLNA	0.022454	LMOD3	0.002115	HRG	0.000825	FZD10	0.002374	CAPN6	1.56E-07
RGS13	0.004554	LOC100507537	0.0192	HSD17B13	6.47E-06	GABRE	5.54E-06	CAPN9	6.36E-09
RGS20	0.014924	LOC101926913	0.006126	HSPB7	0.006969	GABRR1	0.000115	CAPS	9.60E-06
RGS5	0.002111	LRRIQ3	0.006778	HTR3A	0.007845	GAL	0.000167	CAPS2	5.14E-06
RHOJ	0.007548	LY6D	0.000483	IGF2BP3	0.002028	GALNT14	5.06E-06	CAPSL	6.69E-06
ROR1	0.00245	LY6G6C	0.001079	IL1A	0.00057	GALNT16	0.000357	CARD11	0.000379
RPTN	0.047243	LYPD3	5.31E-07	IL1B	0.000559	GAST	1.62E-07	CARD14	3.81E-08
RRM2	0.002756	MAATS1	0.023807	IL1RN	2.59E-05	GATA5	0.011554	CARD18	0.04468
RSPO3	0.003616	MAB21L3	0.001096	IL23A	1.24E-05	GDA	0.000101	CASC1	4.75E-06
RTKN2	0.001313	MALL	0.001586	IL2RA	0.00129	GDF10	0.000358	CASC9	4.83E-09
RUNX1T1	0.001852	MAP2K7	0.002026	IL36G	7.24E-06	GDPD2	0.003169	CASQ2	6.02E-08
S100A2	0.009689	MBOAT2	2.67E-06	IL36RN	0.000136	GINS1	0.004085	CAST	3.32E-11
S100A7	0.004375	MCM10	1.29E-05	IL6	0.015132	GINS2	2.43E-07	CATSPERD	2.96E-05
S100A8	0.004738	MELK	0.000142	INSL4	0.004683	GINS4	1.54E-05	CC2D2A	6.60E-06
S100A9	0.004738	MKI67	0.002087	IQUB	0.016789	GJA3	0.000211	CCDC113	5.44E-05
SBSPON	0.018138	MND1	6.38E-06	ITGBL1	0.005489	GJB6	4.68E-08	CCDC146	0.000613
SCARA5	0.004947	MORN5	0.022179	IVL	0.000243	GNGT1	0.000254	CCDC148	0.000528
SCEL	0.001737	MPP4	0.026247	KCNA1	0.002124	GPM6A	5.55E-07	CCDC150	2.17E-08
SCN2B	0.007564	MREG	8.19E-05	KCNA4	0.002351	GPNMB	9.40E-06	CCDC151	1.85E-05
SCN7A	0.01434	MROH9	0.023937	KCNB1	0.000604	GPR19	3.42E-05	CCDC153	4.06E-06
SDCBP2	0.001313	MS4A2	0.000956	KCNG3	0.000482	GPR87	0.00012	CCDC158	3.61E-07
SEMA3D	0.008221	MSRB3	0.008117	KCNJ1	7.05E-05	GPRC5D	0.00118	CCDC17	2.33E-05
SERPINB2	0.003616	MYBL2	3.26E-06	KCNK10	0.001235	GPX2	0.000162	CCDC170	3.59E-05
SERPINB5	0.002722	MYEF2	0.000859	KCNMB2	0.049887	GREM2	0.000355	CCDC177	5.29E-06
SFRP4	0.0048	MYEOV	0.001308	KCNN3	3.41E-05	GRHL3	8.35E-06	CCDC178	4.00E-12
SGCE	0.003482	MYH11	0.013133	KCTD16	7.43E-05	GRIA2	0.002793	CCDC181	5.25E-05
SH2D1B	0.002907	MYLK	0.001278	KHDRBS2	0.002615	GRID2	0.004978	CCDC187	1.27E-05

SIGLEC17P	0.001979	MYOC	0.031076	KIAA0101	2.82E-06	GRP	0.000663	CCDC189	4.85E-05
SKA1	0.022993	MYOZ2	0.002725	KIAA0408	0.005963	GSDMC	0.001241	CCDC190	0.000498
SLC7A11	0.005466	NAP1L3	0.007075	KIAA1524	0.000226	GSG2	6.93E-07	CCDC38	0.000432
SMOC2	0.00335	NAV3	0.008705	KIAA1549L	0.01343	GSTM1	5.54E-05	CCDC39	8.14E-05
SORBS1	0.01382	NCAPG	3.90E-06	KIF11	3.67E-05	GSTM3	2.37E-05	CCDC65	3.86E-06
SOX5	0.004413	NDC80	0.000875	KIF14	0.001644	GSTM5	7.58E-06	CCDC74B	8.16E-05
SPARCL1	0.002265	NECAB1	0.00084	KIF15	2.65E-05	GTSE1	9.18E-07	CCDC78	5.81E-05
SPC24	0.003653	NETO2	8.72E-05	KIF18A	0.000638	HAND2-AS1	0.005868	CCDC89	6.50E-06
SPC25	0.003448	NMRAL1P1	0.001404	KIF20A	0.000125	HAPLN1	0.007864	CCDC96	1.11E-05
SPON1	0.0173	NMU	5.42E-06	KIF23	9.06E-07	HAS3	2.28E-06	CCL15	1.43E-12
SPRR1A	0.00298	NMUR1	0.000922	KIF2C	3.25E-05	HCK	2.13E-05	CCL18	4.48E-06
SPRR1B	0.001809	NOS1	0.002814	KIF4A	0.000628	HIF3A	0.003602	CCL20	8.30E-05
SPRR2C	0.005676	NPAS3	0.000695	KIFC1	1.91E-05	HIST1H3B	6.43E-05	CCL23	1.90E-05
SPRR2D	0.006174	NUF2	7.05E-05	KIRREL2	0.002827	HIST1H3D	1.34E-05	CCL28	9.82E-05
SPRR2G	0.031496	NUSAP1	5.29E-06	KLF3-AS1	5.84E-05	HJURP	0.000483	CCL3	0.000182
SPRR3	0.002059	OGN	0.033168	KLHL32	0.004478	HLF	0.000105	CCL3L3	8.91E-05
SRGN	0.012409	OIP5	1.96E-05	KLK13	0.015257	HMGA2	0.002027	CCL7	1.41E-05
SSTR1	0.023518	OMD	0.01354	KLK7	0.001195	HMGCS1	1.14E-05	CCL8	7.29E-05
SYNPO2	0.006386	ORC1	0.001489	KLK8	4.55E-05	HMMR	0.000319	CCNA2	3.58E-10
TBX2	0.003214	ORC6	0.000241	KNL1	0.000198	HOXA10	0.000124	CCNB1	3.78E-07
TBX5	0.013875	OVOL1	0.000118	KRT16	1.26E-06	HOXA11-AS	2.93E-06	CCNB2	1.16E-09
TBX5-AS1	0.005083	OXTR	0.036544	KRT16P3	2.48E-05	HOXA13	1.63E-05	CCNE1	4.03E-12
TGM5	0.004994	PADI1	0.000958	KRT24	0.003255	HOXA9	2.59E-06	CCNE2	2.37E-07
TICRR	0.003653	PBK	1.29E-05	KRT34	0.000311	HOXC13	5.36E-08	CCNF	1.93E-08
TMPRSS11A	0.040151	PDLIM3	0.019809	KRT6B	1.16E-07	HOXC9	0.00021	CCNO	2.63E-06
TMPRSS11B	0.008377	PDZRN3	0.004987	KRT6C	6.63E-07	HOXD10	5.01E-07	CCNYL1	1.11E-11
TMPRSS11E	0.004474	PDZRN4	0.001035	KRT75	0.015137	HOXD11	1.10E-06	CCR1	1.84E-07
TNFRSF17	0.027407	PGM5	0.007394	KRT79	0.036384	HPN	0.010357	CCR3	0.008151
TOP2A	0.018934	PGR	0.002529	KRTAP19-1	0.011958	HPSE	5.32E-05	CD163	5.69E-06
TPSAB1	0.001344	PHLDA2	5.29E-06	KRTAP4-1	0.001963	HRCT1	0.008976	CD163L1	0.000435
TPX2	0.018079	PI16	7.20E-05	KRTDAP	0.003795	HRG	1.20E-06	CD1A	0.00034
TTK	0.00315	PI3	0.010175	LAD1	1.01E-05	HS6ST2	0.000474	CD274	1.57E-10
UBE2C	0.005984	PKMYT1	3.87E-06	LAIR2	0.000424	HSD17B13	0.001232	CD300C	1.87E-05
UCA1	0.028829	PKP1	0.000426	LCAL1	8.04E-05	HSPB7	0.001323	CD34	0.00028
UGT2B17	0.013189	PLK1	4.04E-06	LCE3D	8.37E-05	HTR3A	0.004576	CD68	2.79E-09
ULBP2	0.001809	PLN	0.014757	LEPR	0.000366	IDO1	0.032391	CD70	2.13E-06
UPK1B	0.023455	PMCH	0.004543	LHX2	0.003835	IGF2BP3	1.23E-07	CD80	8.38E-10
VCAM1	0.011486	PMP2	0.002029	LILRA5	0.004638	IGFBP6	0.000446	CD84	0.000181
WISP1	0.006901	PNMAL1	0.000763	LINC00491	0.001503	IGSF3	1.60E-05	CDC20	6.98E-08
XIST	0.030367	POLQ	0.000197	LINC00643	0.007248	IL17D	0.000368	CDC25A	7.27E-08

ZBED2	0.015494	PPIL6	0.025247	LINC01206	0.007645	IL1A	0.000215	CDC25C	1.03E-05
ZFPM2	0.001797	PPP1R1A	0.001254	LINC01589	0.006485	IL1B	4.89E-05	CDC45	1.35E-12
ZNF521	0.005508	PPP2R2C	0.000152	LINC01615	0.011169	IL1RAP	3.26E-06	CDC6	2.05E-13
ZWINT	0.001705	PRC1	9.30E-06	LIPG	0.003622	IL1RN	1.78E-06	CDCA2	9.15E-10
		PRR29	0.018888	LMO3	0.000669	IL2RA	0.000125	CDCA3	5.04E-11
		PRSS2	4.81E-07	LMOD1	0.005766	IL33	7.77E-05	CDCA4	1.38E-07
		PRSS27	0.000807	LOC100129516	0.001091	IL36G	1.38E-07	CDCA5	1.48E-12
		PRSS3	1.22E-07	LOC100507311	1.47E-06	IL36RN	5.58E-07	CDCA7	1.31E-08
		PRSS35	0.001814	LOC100507537	0.016752	IRX4	0.017509	CDCA8	8.53E-11
		PRUNE2	0.010444	LRRIQ3	0.004842	ISL1	0.000612	CDCP1	8.36E-06
		PTCHD1	0.038684	LY6G6C	0.000759	ITGA8	0.002554	CDH12	2.18E-05
		PTGFR	0.002924	LY6K	0.001193	ITGBL1	0.00218	CDH19	3.24E-10
		PTPRH	0.004672	LYPD3	1.57E-05	ITLN1	0.021628	CDH24	1.52E-08
		PTTG1	1.07E-05	MACROD2	5.45E-05	IVL	2.27E-05	CDH26	2.21E-05
		PTTG2	1.29E-05	MADCAM1	0.001267	IZUMO1	0.000128	CDHR3	2.00E-05
		PTTG3P	8.72E-05	MAGEA9	0.027983	JAM2	0.003914	CDK1	1.28E-08
		RAB38	7.05E-05	MAGI2-AS3	0.000146	JCHAIN	0.018262	CDK5R1	2.40E-06
		RACGAP1	1.14E-05	MALL	0.004505	JPH2	0.00031	CDKN2A	2.51E-06
		RAD51	7.08E-06	MAP7D2	0.005465	KANK4	0.009794	CDKN2B	4.57E-06
		RAD54L	1.69E-05	MCEMP1	0.027734	KCNA4	0.001755	CDKN3	4.77E-11
		RBM24	0.031618	MCM10	1.18E-05	KCNA5	0.038335	CDNF	3.39E-10
		RDH12	0.002924	MELK	1.15E-05	KCNG3	1.92E-05	CDO1	3.65E-05
		RGS13	0.002625	MKI67	0.000521	KCNJ1	0.001725	CDT1	3.98E-10
		RGS20	0.002135	MMP12	0.000237	KCNJ5	0.000269	CDX1	1.33E-07
		RGS4	0.003113	MMP9	0.002841	KCNK10	0.009887	CDYL2	4.93E-05
		RHCG	0.000461	MND1	2.18E-06	KCNMB2-AS1	0.00013	CENPA	1.10E-08
		RP1	0.033264	MPP4	0.010149	KCTD16	0.00027	CENPE	8.14E-10
		RPTN	0.007077	MREG	5.17E-05	KHDRBS2	0.000158	CENPF	1.38E-11
		RRM2	1.21E-05	MROH9	0.015325	KIAA0101	2.96E-07	CENPI	6.23E-07
		RSPO3	0.012398	MYBL2	5.86E-07	KIAA1524	1.86E-05	CENPK	9.45E-07
		RTKN2	1.39E-06	MYH11	0.011611	KIAA1549L	0.00035	CENPL	1.43E-12
		S100A12	0.007177	MYOC	0.000662	KIF11	1.47E-05	CENPM	1.93E-09
		S100A14	0.000116	NCAPG	2.34E-06	KIF14	0.000267	CENPN	9.57E-12
		S100A2	1.14E-05	NDC80	0.000199	KIF15	2.82E-05	CENPP	9.73E-09
		S100A7	2.66E-05	NECAB1	0.000451	KIF18A	0.000212	CENPU	2.06E-10
		S100A7A	0.038329	NEFL	0.029843	KIF20A	0.000905	CENPW	9.17E-08
		S100A8	1.69E-05	NEGR1	8.45E-05	KIF23	2.89E-07	CEP126	5.39E-06
		S100A9	2.35E-05	NEIL3	0.002049	KIF2C	7.82E-06	CEP55	2.79E-09
		SAMD9	3.20E-05	NET02	1.23E-05	KIF4A	7.79E-05	CERK	1.11E-09
		SBSPON	0.006624	NKAIN2	0.017644	KIFC1	2.41E-06	CERS3	0.028814

SCARA5	0.020035	NMRAL1P1	3.24E-06	KLF3-AS1	0.000605	CFAP100	7.43E-05
SCEL	2.87E-06	NMU	0.001692	KLK7	0.001639	CFAP126	4.53E-05
SCGB1A1	0.004336	NOS1	0.002589	KLK8	2.56E-05	CFAP157	7.12E-05
SCN2B	0.00146	NPAS3	8.94E-05	KLRG2	0.000177	CFAP161	1.80E-05
SCN7A	0.013498	NPL	6.77E-07	KNL1	4.48E-06	CFAP206	5.85E-05
SDCBP2	1.29E-05	NR2F2-AS1	1.04E-05	KRT13	0.030218	CFAP221	9.59E-06
SEMA3D	0.005663	NSUN7	0.001576	KRT16	2.53E-09	CFAP43	8.36E-06
SERPINB13	0.000709	NTRK2	0.000491	KRT16P3	7.55E-08	CFAP45	3.42E-05
SERPINB2	8.78E-05	NUF2	8.17E-06	KRT222	4.97E-05	CFAP46	2.00E-05
SERPINB5	2.66E-06	NUSAP1	5.42E-06	KRT24	0.001845	CFAP47	1.48E-05
SERPINB8	2.82E-05	OGN	0.01501	KRT34	0.001202	CFAP52	1.57E-05
SFN	3.07E-05	OIP5	1.01E-06	KRT5	0.000651	CFAP53	0.001516
SGO1	0.000109	ORC1	0.007962	KRT6B	5.46E-10	CFAP54	0.002604
SH2D1B	3.52E-05	ORC6	7.24E-06	KRT6C	8.21E-09	CFAP61	2.65E-05
SHCBP1	0.000372	OSBPL6	0.00274	KRT75	0.001042	CFAP65	1.55E-05
SIGLEC17P	0.002101	OVOL1	0.000214	KRT77	0.001896	CFAP69	9.51E-06
SKA1	0.001016	OXTR	0.008669	KRT78	0.004078	CFAP70	2.40E-06
SKA3	4.31E-05	PBK	2.55E-05	KRT79	0.004156	CFH	6.43E-08
SLC13A5	0.007136	PCAT7	0.005333	KRT80	4.49E-06	CFHR4	6.44E-05
SLC16A12	0.001688	PCSK1	0.019654	KRTAP4-1	3.98E-08	CFTR	1.28E-08
SLC39A2	0.000323	PCSK9	0.018496	KRTDAP	0.000252	CH25H	0.000325
SLC6A13	0.001155	PDE4DIP	0.001344	LAD1	6.47E-07	CHAC2	8.60E-11
SLC7A11	0.020086	PDE5A	0.000635	LAIR2	0.001552	CHEK1	4.35E-12
SLC7A5	0.000346	PDLIM3	0.030005	LCAL1	1.53E-07	CHGB	0.000276
SLC9C2	0.009343	PDZRN4	0.000178	LCE2B	0.00054	CHI3L1	8.72E-06
SLITRK3	0.005057	PGBD5	0.000496	LCE2C	0.000237	CHIT1	0.000217
SLURP1	0.003239	PGM5	0.000264	LCE3A	0.001668	CHL1	2.33E-09
SMOC2	0.00303	PGM5P4-AS1	0.000534	LCE3D	5.18E-07	CHODL	0.000368
SORBS1	0.002671	PGR	0.004006	LEMD1	0.004973	CHRDL1	2.63E-07
SOX5	0.000815	PHLDA2	1.71E-05	LEPR	0.000137	CHRM3	0.00533
SPAG6	0.036248	PI16	3.17E-05	LGI1	0.003252	CHRNA3	0.000287
SPARCL1	0.003982	PI3	0.000369	LHX2	7.98E-05	CHRNA5	5.10E-08
SPATA19	0.00289	PIF1	3.17E-05	LINC00491	6.16E-06	CHST6	9.48E-07
SPATS1	0.022652	PITX2	0.007236	LINC00844	0.001372	CHST9	1.83E-13
SPC24	0.000142	PKMYT1	2.10E-06	LINC01206	0.000281	CILP	0.000875
SPC25	3.87E-06	PKP1	0.000312	LINC01354	0.000188	CKAP2L	6.58E-07
SPINK6	0.012714	PLA2G7	0.000144	LINC01589	0.001417	CKMT2	4.63E-09
SPRR1A	1.33E-06	PLAC1	0.001267	LINC01615	8.01E-05	CKS2	6.38E-11
SPRR1B	7.82E-08	PLAU	0.000134	LIPG	0.001164	CLCA3P	0.024393
SPRR2C	1.22E-07	PLAUR	4.52E-05	LMOD1	0.000439	CLCN5	4.79E-07

SPRR2D	7.72E-07	PLCH1	0.000506	LOC100129516	0.00101	CLDN10	0.000202
SPRR2E	3.46E-05	PLK1	2.10E-06	LOC100507311	8.58E-07	CLDN22	0.000883
SPRR2G	0.004491	PLN	0.006558	LOC149351	0.000121	CLDN3	9.59E-08
SPRR3	1.97E-06	POLE2	0.002486	LOC284244	8.32E-05	CLEC12A	0.000181
SSPN	2.31E-05	POLQ	0.000288	LOC349160	0.000484	CLEC3B	4.04E-06
STOML3	0.035672	PPP1R1A	0.002763	LRCH2	0.002185	CLEC4D	4.84E-05
SYNE1	0.006409	PPP1R3C	0.000635	LRRC2	7.96E-05	CLEC4E	6.83E-05
SYNM	0.003817	PPP2R2C	0.000153	LY6G6C	0.000333	CLEC5A	1.02E-05
SYNPO2	0.004505	PRAME	0.002591	LY6K	2.98E-05	CLEC7A	4.13E-08
TEKT3	0.01875	PRC1	2.44E-06	LYPD3	1.48E-06	CLIC5	7.84E-06
TEX26	0.009385	PRDM13	0.003991	MAB21L3	0.000887	CLIC6	2.69E-10
TGM5	0.001974	PRDM16	0.000111	MADCAM1	0.002245	CLIP4	1.16E-06
THBS4	0.004293	PROK2	0.042726	MAGEA12	0.000478	CLMN	4.82E-08
TICRR	1.03E-06	PROS1	0.000345	MAGEA2B	0.001402	CLSPN	7.30E-06
TK1	6.12E-06	PRSS2	0.00011	MAGEA4	0.025473	CLUL1	2.88E-11
TMEM108	0.001429	PRSS3	6.47E-05	MAGEA9	0.006382	CMAHP	3.36E-10
TMEM79	4.89E-06	PRUNE2	0.000867	MALL	4.53E-06	CMTM3	1.09E-05
TMPRSS11A	0.011305	PTCHD1	0.008995	MAP7D2	0.015711	CMYA5	4.46E-07
TMPRSS11B	0.002856	PTGFR	0.001788	MAPK4	0.000416	CNGB3	1.39E-06
TMPRSS11D	0.00159	PTHLH	5.04E-05	MCEMP1	0.029573	CNN1	5.67E-06
TMPRSS11E	0.006053	PTTG1	1.87E-05	MCM10	5.23E-06	CNTD1	6.36E-09
TNN	0.030418	PTTG2	3.31E-05	MCM2	2.53E-09	CNTN2	0.000836
TNNT1	0.001357	PTTG3P	4.41E-05	MELK	1.27E-05	CNTN3	4.17E-05
TOP2A	0.000221	RACGAP1	1.12E-05	MELTF	0.000125	CNTN4	1.44E-05
TOX	0.000332	RAD51	1.75E-07	MEOX2	0.003122	CNTNAP2	1.85E-05
TPM2	0.007545	RAD51AP1	8.04E-05	MFAP4	0.001336	COBL	2.71E-07
TPX2	0.000162	RAD54L	1.66E-06	MGC24103	4.31E-05	COCH	2.64E-09
TRIM7	6.47E-05	RCAN2	0.001956	MGP	2.82E-05	COL10A1	2.82E-06
TROAP	4.99E-06	RERGL	0.001658	MIR100HG	0.002949	COL11A1	1.65E-06
TSPAN2	0.012473	RGS20	3.57E-05	MKI67	0.000315	COL14A1	2.85E-07
TTK	3.46E-05	RHCG	0.002572	MKRN3	0.00568	COL21A1	1.52E-11
TUBB4A	0.001159	RNASE2	0.014748	MMP1	0.00041	COL3A1	0.00046
TXN	7.06E-05	RP1	0.038611	MMP12	1.00E-06	COL4A1	8.87E-06
TYMS	6.82E-05	RPTN	0.044733	MMP3	0.000949	COL4A6	1.01E-08
TYMSOS	0.000482	RRM2	5.09E-06	MMP9	0.00027	COL5A2	5.85E-05
UBE2C	1.97E-06	RTKN2	0.000123	MND1	5.43E-08	COLEC11	2.67E-08
UCA1	0.00047	RYR3	0.017864	MREG	4.28E-06	COMP	0.003681
UGT1A8	0.012729	S100A12	0.000897	MSRB3	0.001476	CORIN	2.57E-05
UHRF1	7.71E-05	S100A2	0.009695	MYBL2	1.68E-08	CORO1C	8.65E-12
ULBP2	2.38E-06	S100A7	4.24E-06	MYC	0.000203	CORO2B	8.35E-08

UNC45B	0.011862	S100A7A	0.000316	MYH11	0.00914	COTL1	5.33E-08
UPK1B	0.013235	S100A8	0.000149	MYLK	0.004576	COX7A1	1.85E-05
WDR72	0.012591	S100A9	0.000142	MYOC	1.10E-05	CPA6	2.47E-06
WFDC5	0.006979	SAPCD2	5.72E-05	MYOT	0.001805	CPAMD8	1.03E-12
XKR4	0.033382	SBSPON	0.034219	NAMPT	1.11E-06	CPEB1	3.64E-06
ZBED2	0.000102	SCARA5	0.017731	NAP1L3	0.001561	CPED1	5.01E-06
ZWINT	9.65E-07	SCEL	0.000367	NCAPG	3.26E-06	CPNE7	8.14E-09
		SCGB1A1	1.77E-05	NDC80	0.000856	CPXM1	4.26E-05
		SCGB3A1	0.002541	NDN	4.15E-05	CPZ	0.002577
		SCN2B	0.000382	NDRG4	4.60E-06	CRB1	0.000331
		SCN7A	0.0004	NEB	0.000144	CRCT1	0.009026
		SEC14L3	0.000199	NECAB1	9.43E-06	CREG1	3.89E-11
		SEMA3E	0.013926	NEFL	0.021276	CRIP1	6.69E-07
		SERPINB13	0.004734	NEGR1	0.000925	CRISP2	2.30E-05
		SERPINB2	0.003253	NEIL3	0.000167	CRLF1	1.93E-05
		SERPINB5	0.000295	NEK2	0.002454	CRY2	1.51E-12
		SFN	0.000151	NETO2	2.96E-05	CRYM	5.62E-08
		SFRP4	0.01335	NEURL3	1.81E-06	CSAG1	1.45E-05
		SGO1	0.000111	NEXN	0.008352	CSAG3	0.00109
		SHCBP1	0.00011	NKAIN2	7.60E-05	CSF2	3.83E-12
		SKA1	0.000143	NMRAL1P1	3.72E-11	CSH1	5.86E-08
		SKA3	1.53E-05	NMU	0.015847	CSTA	0.000715
		SLC13A5	0.003411	NPL	1.42E-08	CT45A5	5.93E-05
		SLC16A1	1.97E-05	NR2F2-AS1	6.89E-06	CTHRC1	2.89E-07
		SLC16A12	7.36E-05	NRG2	3.46E-05	CTLA4	1.85E-06
		SLC23A1	0.013205	NTNG1	0.001473	CTSB	1.20E-07
		SLC2A5	0.001562	NTRK2	7.81E-07	CTSL	1.59E-06
		SLC35F3	0.00603	NTS	0.036098	CTSV	0.00011
		SLC38A11	0.008467	NUF2	7.26E-07	CUL3	3.62E-09
		SLC39A2	0.005993	NUSAP1	3.99E-07	CXCL12	0.000141
		SLC6A13	0.009324	OAS2	5.77E-05	CXCL13	8.70E-06
		SLC7A11	0.000255	OGN	0.000184	CXCL3	0.001912
		SLC7A5	3.56E-05	OIP5	1.10E-06	CXCL5	5.60E-08
		SLC9C2	0.008461	OLFM4	0.003924	CXCL9	0.034998
		SLIT2	0.000476	OMD	0.007977	CXCR2P1	0.000221
		SLITRK3	0.037974	ORC1	0.001795	CXXC4	1.04E-08
		SLITRK6	1.20E-05	ORC6	3.98E-07	CYBB	5.76E-06
		SMC4	5.86E-07	OSM	0.000676	CYBRD1	6.74E-06
		SMOC2	0.015103	OSMR	1.12E-05	CYP26A1	0.004464
		SNX29P2	0.000139	OVOL1	9.19E-05	CYP27B1	8.64E-11

SORBS1	0.001974	P2RY1	4.03E-05	CYP2A13	6.38E-10
SOST	0.000179	PBK	2.20E-05	CYP2A6	2.88E-06
SOX5	0.000324	PCAT7	1.88E-05	CYP2A7	3.25E-06
SPC24	0.00019	PCDH10	0.001001	CYP2B6	1.48E-08
SPC25	4.24E-06	PCDH8	0.006111	CYP2B7P	2.78E-06
SPINK1	0.013995	PCOLCE2	0.017051	CYP2F1	2.75E-12
SPINK6	0.019254	PCSK1	0.001092	CYP2J2	1.35E-12
SPRR1A	1.59E-05	PCSK2	0.003119	CYP4B1	1.02E-10
SPRR1B	5.86E-07	PCSK9	8.47E-06	CYP4F11	0.002109
SPRR2C	6.63E-07	PDE5A	0.000895	CYP4X1	1.00E-06
SPRR2D	8.39E-07	PDLIM3	0.016278	CYYR1	1.58E-05
SPRR2E	4.00E-05	PDZRN3	9.25E-05	DACH1	0.000781
SPRR2G	9.08E-06	PDZRN4	1.24E-05	DACH2	0.010384
SPRR3	0.000103	PEBP4	0.003096	DACT2	0.000304
SSTR1	0.006313	PER3	5.06E-05	DACT3	6.67E-05
STAR	0.006442	PGBD5	0.002868	DAW1	5.67E-06
STRIP2	0.00014	PGLYRP4	0.00157	DCDC5	0.000588
SULT1B1	0.000112	PGM5	3.22E-05	DDAH1	4.70E-08
SYNE1	0.000115	PGR	1.68E-06	DDC	0.00026
SYNPO2	0.000631	PI16	5.08E-06	DDIAS	1.09E-12
TACC3	1.45E-05	PI3	0.001267	DDIT4L	9.67E-05
TCL1A	0.003983	PIGX	1.42E-08	DEFB103B	1.34E-05
TEX26	0.01362	PITX2	2.45E-06	DEFB126	8.29E-06
TGM5	0.00579	PKMYT1	8.48E-08	DEFB4A	0.000101
TICRR	4.55E-07	PKP1	1.71E-07	DEPDC1	4.33E-07
TK1	1.26E-06	PLA2G7	0.000291	DEPDC1B	7.79E-09
TLR8	0.002286	PLAC1	7.29E-05	DEPTOR	2.08E-07
TM4SF19	0.001531	PLAU	2.65E-07	DES	1.05E-06
TMEM163	0.00019	PLK1	5.18E-07	DEUP1	0.00118
TMPRSS11A	0.014415	PLN	0.000352	DGAT2	2.13E-08
TMPRSS11B	0.021732	PLP1	0.006607	DHFR	1.47E-09
TMPRSS11D	0.004191	PMP2	6.74E-05	DHRS2	4.68E-06
TMPRSS11E	8.54E-05	PNMAL1	0.001483	DHRS9	4.13E-07
TNFRSF9	0.000471	POLE2	0.000455	DHX29	5.29E-07
TNIP3	0.000484	POLQ	3.06E-07	DIAPH3	2.01E-11
TNNT1	1.71E-06	POU4F1	0.000554	DIO3	0.000764
TOP2A	0.000139	PPARGC1A	1.36E-05	DIO3OS	1.20E-06
TPM2	0.010905	PPP1R3C	0.000889	DIRAS2	7.61E-05
TPX2	1.82E-05	PPP2R2C	1.40E-07	DIXDC1	2.26E-09
TRIP13	0.001259	PRAME	1.70E-09	DLG2	1.81E-11

TROAP	1.01E-06	PRB1	0.029292	DLGAP5	3.06E-09
TRPA1	0.001775	PRC1	1.44E-06	DLL3	2.23E-08
TTK	2.00E-05	PRDM13	0.000287	DLX1	7.98E-05
TUBA1C	5.86E-07	PRDM16	9.34E-06	DLX4	2.99E-06
TUBB3	4.32E-05	PRSS2	0.001141	DLX5	6.44E-07
TUBB4A	0.001546	PRSS27	0.003957	DMBT1	0.000783
TYMS	2.82E-05	PRSS3	0.0002	DMD	3.37E-10
TYMSOS	0.00031	PRSS35	0.001257	DMGDH	2.69E-07
UBE2C	1.26E-06	PRUNE2	0.013027	DMRT3	7.66E-10
UCA1	0.02969	PTCHD1	0.027268	DMRTA1	7.84E-07
UHRF1	1.53E-05	PTGFR	0.000759	DMRTC1	1.65E-12
ULBP2	7.03E-06	PTGIS	0.0022	DNA2	6.92E-07
USH1G	0.000556	PTTG1	1.60E-05	DNAH12	4.46E-06
UTS2	0.0166	PTTG2	7.41E-05	DNAH17	8.06E-08
VGLL3	0.006588	PTTG3P	6.09E-05	DNAH2	6.78E-05
VIT	0.017199	QRFPR	0.000526	DNAH3	0.000595
VSNL1	0.001229	RACGAP1	4.72E-06	DNAH5	0.00024
WDR72	0.000109	RAD51	1.56E-08	DNAH6	6.12E-06
WFDC5	0.002004	RAD51AP1	1.50E-05	DNAH7	4.15E-07
ZBED2	1.73E-05	RAD54L	9.75E-09	DNAH9	4.47E-06
ZBTB32	0.00683	RBMS3	2.72E-06	DNAI1	2.84E-05
ZFPM2	0.00596	RCAN2	6.14E-05	DNAI2	4.60E-05
ZIC5	0.0023	REG1A	1.69E-05	DNALI1	1.15E-05
ZNF295-AS1	0.017348	RERG	1.34E-05	DNER	4.82E-05
ZNF695	0.001554	RERGL	0.000296	DOCK2	3.21E-05
ZWINT	5.86E-07	RFC4	2.53E-09	DOCK3	0.000391
		RFLNA	0.001872	DPP10-AS1	2.63E-05
		RGS20	0.000412	DPT	3.87E-05
		RHCG	1.63E-06	DPY19L2	4.06E-06
		RMI2	4.62E-06	DPY19L2P2	2.45E-05
		RNASE2	0.003159	DPY19L2P4	1.39E-06
		ROR1	0.000388	DQX1	0.000443
		RORC	0.0002	DRC1	6.79E-06
		RPTN	0.006113	DRC3	9.24E-06
		RRM2	2.91E-05	DRC7	0.000156
		RSPO3	0.003972	DSC1	4.23E-05
		RTKN2	0.000473	DSC2	9.66E-11
		RUNX1T1	0.002193	DSC3	0.003845
		S100A12	0.000167	DSCC1	5.04E-07
		S100A2	0.017271	DSG3	1.87E-07

S100A7	1.88E-07	DSP	0.000428
S100A7A	0.00032	DTL	1.05E-12
S100A8	9.18E-07	DUSP12	5.46E-07
S100A9	9.01E-06	DUSP26	4.16E-08
SAMD9	9.49E-05	DUSP5P1	2.49E-06
SBSPON	0.004955	DUXAP10	8.85E-06
SCARA5	1.41E-05	DUXAP8	1.16E-09
SCD	2.93E-05	DYDC1	3.44E-05
SCEL	0.004031	DYDC2	0.000221
SCGB1A1	0.000248	DYNC1I1	0.000142
SCGB3A1	0.000171	DYNC2H1	1.11E-05
SCGN	0.000282	DYNLRB2	2.57E-06
SCN2B	6.68E-07	DYX1C1	9.47E-05
SCN3A	0.000685	DZIP3	0.000368
SCN7A	6.14E-06	E2F1	2.13E-13
SCN9A	0.000514	E2F2	5.20E-09
SCRG1	0.038597	EBF1	0.000531
SENP5	1.06E-09	ECE2	2.01E-11
SERPINB13	0.003448	ECEL1	8.35E-06
SERPINB2	0.022358	ECT2	2.78E-11
SERPINB5	5.85E-05	ECT2L	0.000142
SFN	1.68E-05	EDN2	1.22E-05
SFRP4	0.00628	EDNRB	5.63E-06
SFTA3	0.000698	EEF1A2	1.76E-05
SGK1	3.06E-06	EEF1D	2.79E-08
SH2D1B	0.015045	EFCAB1	7.98E-06
SH2D5	0.000301	EFCAB6	1.04E-05
SHCBP1	2.25E-05	EFCC1	7.39E-07
SHOX2	5.23E-05	EFEMP1	4.11E-08
SKA1	0.000222	EFHB	2.38E-06
SKA3	6.82E-05	EFHC1	1.15E-05
SLC12A8	0.000144	EFHC2	3.34E-05
SLC16A12	4.55E-06	EFHD1	2.09E-11
SLC22A16	0.016169	EGFEM1P	0.000839
SLC26A4	0.022744	EGLN3	2.96E-06
SLC30A3	3.33E-05	EGR4	0.000101
SLC35F1	0.004193	EHF	7.12E-08
SLC35F3	0.000482	EIF5A2	3.30E-09
SLC39A2	2.85E-06	ELF5	3.65E-05
SLC44A5	0.000307	ELN	5.97E-07

SLC6A10P	2.76E-07	EMCN	2.22E-05
SLC7A11	2.84E-06	EME1	8.28E-09
SLC7A5	5.29E-07	EN1	9.78E-07
SLIT2	0.000843	ENKUR	5.45E-05
SLITRK3	0.024678	ENPP3	3.17E-09
SLITRK6	1.70E-06	ENPP4	8.65E-08
SLPI	0.003319	EPHA3	4.96E-05
SMC4	5.43E-09	EPHA5-AS1	0.000114
SMOC2	0.006776	ERBB4	4.64E-10
SOD2	9.42E-07	ERC2	1.06E-07
SORBS1	0.000421	ERCC6L	1.60E-06
SOST	6.13E-07	ERICH3	1.76E-06
SOX10	0.000505	ERICH5	4.09E-05
SOX5	0.000977	ERICH6	3.11E-05
SPARCL1	0.000284	ERO1A	1.36E-13
SPC24	0.000381	ERVMER34-1	7.56E-08
SPC25	5.18E-07	ESCO2	1.91E-09
SPERT	0.000103	ESPL1	5.44E-11
SPINK1	0.012967	ESRRG	3.97E-07
SPOCD1	0.001202	ETV1	1.35E-05
SPP1	0.000612	EXO1	1.07E-10
SPRR1A	5.18E-07	EYA1	2.10E-13
SPRR1B	1.88E-07	EYA4	6.36E-09
SPRR2C	1.53E-09	EZH2	9.16E-12
SPRR2D	1.08E-08	F3	1.88E-09
SPRR2E	8.35E-06	FABP5	1.19E-09
SPRR2G	5.69E-09	FADS1	9.16E-09
SPRR3	3.04E-06	FADS2	1.58E-05
SRPX	0.008755	FAM107A	3.67E-13
SRXN1	1.11E-06	FAM111B	1.01E-06
SSTR1	0.000284	FAM120A	4.81E-06
STAR	0.001725	FAM126A	1.29E-08
STC2	0.000381	FAM149A	1.29E-08
STMN2	0.00482	FAM150A	4.09E-05
SULT1B1	0.000193	FAM150B	0.001933
SVEP1	0.000241	FAM162B	1.54E-05
SYNE1	0.00288	FAM174B	1.81E-12
SYNPO2	0.000711	FAM183BP	1.53E-05
SYT14	0.000223	FAM189A2	3.40E-10
TCEAL2	0.002022	FAM19A2	4.04E-05

TCL1A	0.014568	FAM20C	4.81E-05
TDH	0.001381	FAM216B	0.000168
TDO2	0.000343	FAM221A	1.68E-10
TFRC	1.41E-09	FAM225A	3.52E-06
TGM5	0.000649	FAM228A	3.92E-07
TICRR	2.56E-09	FAM229B	1.24E-05
TIMELESS	1.28E-08	FAM3B	1.94E-07
TIMP3	5.08E-06	FAM3D	1.47E-11
TK1	2.56E-09	FAM46C	8.14E-06
TMEFF2	0.005846	FAM47E	1.69E-06
TMEM100	0.002806	FAM49A	2.80E-07
TMEM163	0.000127	FAM64A	5.77E-07
TMEM47	0.000234	FAM65B	0.000636
TMEM79	1.32E-06	FAM72D	4.40E-11
TMPRSS11A	8.36E-05	FAM81B	8.73E-06
TMPRSS11B	0.00492	FAM83A	7.30E-06
TMPRSS11D	0.000737	FAM83B	1.46E-09
TMPRSS11E	1.91E-06	FAM83C	0.000687
TMPRSS11F	0.000222	FAM89A	7.88E-08
TNFRSF9	0.000123	FAM92B	5.81E-06
TNIP3	4.63E-06	FANCA	5.80E-13
TNNT1	3.33E-06	FANCB	1.07E-07
TONSL	3.94E-06	FANCI	3.50E-12
TOP2A	0.000122	FANK1	0.000125
TPM2	0.00288	FAP	0.003368
TPTE2P6	0.000368	FASN	3.58E-08
TPX2	1.11E-06	FAXDC2	2.99E-13
TRIM59	1.88E-05	FBLN1	0.000129
TRIP13	0.002095	FBN2	0.001152
TROAP	1.42E-08	FBXL13	9.87E-06
TRPC1	3.89E-07	FBXO15	6.16E-06
TTK	9.24E-07	FBXO36	1.79E-05
TUBA1C	7.55E-08	FBXW10	3.23E-05
TUBB3	2.46E-05	FCGBP	0.007188
TYMS	4.39E-05	FCGR1B	9.48E-05
TYMSOS	0.001872	FCGR2A	2.32E-06
UBE2C	5.80E-07	FCGR3A	0.000219
UBE2T	6.53E-07	FCGR3B	5.72E-06
UCA1	0.002535	FCRLB	6.00E-07
UCHL1	0.006479	FEN1	2.19E-10

UGT1A6	0.004548	FENDRR	0.000205
UGT1A8	0.001918	FER1L5	8.62E-05
UHRF1	7.13E-07	FGD6	3.13E-12
ULBP2	6.26E-07	FGF14	3.79E-06
UMPS	4.75E-05	FGF7	3.03E-08
VGLL3	0.000621	FGF9	1.17E-08
VIT	0.002893	FGFR2	2.87E-09
VNN1	0.007531	FGR	3.17E-06
WDR72	4.89E-08	FHAD1	1.67E-05
WFDC5	2.47E-05	FHL1	7.00E-07
WISP2	0.000959	FILIP1	5.33E-08
WWTR1	4.89E-08	FKBP4	2.09E-07
XCL1	0.001118	FLAD1	2.16E-09
XCL2	0.000857	FLJ30901	1.84E-07
XIST	0.011418	FLRT3	5.50E-07
XKR4	0.004326	FLVCR2	1.55E-06
ZBED2	4.39E-05	FMN2	4.56E-05
ZBTB16	0.001635	FMO1	0.00014
ZBTB32	0.004746	FMO2	1.24E-10
ZFP64	3.71E-08	FMO3	1.09E-06
ZFPM2	0.000718	FMO5	1.14E-11
ZIC2	0.000614	FNDC3B	3.62E-09
ZIC5	1.71E-07	FOLR1	1.18E-07
ZNF471	1.47E-05	FOSL1	9.76E-05
ZWINT	1.50E-07	FOXA1	2.06E-12
		FOXA2	1.50E-05
		FOXA3	1.60E-05
		FOXJ1	1.26E-05
		FOXL2	5.44E-11
		FOXM1	7.81E-12
		FOXN4	0.002793
		FOXP1	6.89E-11
		FOXRED2	7.61E-10
		FPR1	0.000332
		FPR2	3.69E-05
		FPR3	1.53E-05
		FREM1	2.58E-06
		FRMD1	8.01E-05
		FRMD6	4.54E-05
		FRZB	0.003233

FSCN1	8.64E-10
FXYD1	1.78E-13
FZD4	1.52E-07
G6PD	8.75E-09
GABPB1	3.79E-11
GABRE	7.12E-07
GABRP	1.28E-06
GABRR1	2.87E-06
GAL	3.02E-11
GALNT14	1.48E-08
GALNT16	2.02E-09
GAS2	3.26E-09
GAS2L2	5.00E-06
GAS2L3	1.72E-05
GAS5	7.57E-07
GAST	4.32E-07
GATA5	0.00039
GDF10	1.11E-11
GGT8P	6.65E-07
GINS1	4.98E-08
GINS2	1.01E-11
GINS3	5.74E-06
GINS4	1.35E-12
GIPC2	2.71E-06
GJA1	6.60E-05
GJB1	8.81E-12
GJB2	0.000209
GJB6	5.29E-08
GJC3	0.00081
GLDC	0.001056
GLIPR1L2	3.49E-05
GLYATL1	0.014662
GMDS-AS1	7.87E-09
GMPR	5.44E-08
GMPS	3.37E-11
GNA14	1.41E-05
GNB1	2.93E-10
GNB4	9.49E-09
GNG4	5.52E-05
GNGT1	9.75E-10

GNMT	3.87E-06
GPAT4	2.17E-05
GPIHBP1	2.58E-08
GPM6A	1.51E-12
GPNMB	6.23E-08
GPR158	8.16E-06
GPR162	0.0001
GPR19	3.26E-09
GPR84	1.54E-07
GPRASP1	2.88E-11
GPRC5B	8.12E-09
GPRIN1	1.52E-05
GREM1	1.09E-06
GREM2	7.59E-11
GRHL3	0.0001
GRIA2	0.002291
GRID2	0.000422
GRIN3A	0.000229
GRIN3B	3.99E-05
GRM5	0.005329
GRM7	0.000159
GRM8	4.13E-05
GRP	4.32E-06
GSDMC	0.002009
GSG2	2.11E-10
GSTA1	3.88E-08
GSTA2	6.12E-08
GSTA3	3.63E-07
GSTA5	1.16E-07
GSTM3	0.00166
GSTM5	3.34E-08
GTSE1	3.01E-10
GTSF1	0.000331
GZMB	0.000404
HAB1	1.34E-05
HAND2-AS1	2.02E-05
HCK	2.07E-10
HELB	2.18E-07
HEPACAM2	7.05E-06
HEY2	1.39E-10

HHLA2	0.000428
HIF3A	3.42E-05
HIST1H1B	0.002178
HIST1H2AL	5.10E-05
HIST1H3B	6.55E-07
HIST1H3D	3.43E-07
HIST1H3H	1.76E-07
HIST1H4A	1.93E-05
HJURP	3.55E-06
HK3	2.26E-07
HKDC1	4.91E-05
HLF	5.27E-12
HMGCLL1	3.63E-06
HMGCS1	3.25E-09
HMMR	1.18E-07
HMOX1	1.02E-07
HOXA10	1.11E-11
HOXA11-AS	3.94E-10
HOXA13	5.51E-08
HOXA9	2.51E-09
HOXB13	0.008324
HOXB9	3.98E-06
HOXC13	4.51E-09
HOXC8	1.14E-08
HOXC9	9.05E-10
HOXD10	1.18E-08
HOXD11	1.25E-08
HPCA	2.87E-06
HRASLS2	1.26E-05
HRCT1	0.000187
HRG	2.20E-05
HS3ST3A1	5.38E-06
HSD17B13	5.33E-07
HSD3B7	3.64E-07
HSPB2	0.000237
HSPB7	4.30E-08
HTR2C	2.21E-05
HTRA4	6.21E-09
IBSP	8.24E-09
ICA1L	1.51E-05

IDO1	0.011587
IFI30	1.95E-07
IFNG	0.008705
IFT57	8.87E-06
IFT88	1.07E-06
IGDCC4	0.004389
IGF2BP3	2.83E-11
IGFBP3	8.55E-08
IGFL2	5.18E-06
IGHG1	0.005765
IGSF10	1.43E-08
IGSF22	4.31E-07
IGSF3	2.00E-05
IGSF6	0.0002
IL10	5.33E-08
IL17RD	1.82E-08
IL1A	3.37E-08
IL1B	2.48E-07
IL1RAP	1.44E-10
IL1RN	3.36E-06
IL23A	3.29E-08
IL24	9.64E-07
IL2RA	8.47E-10
IL33	6.65E-11
IL36G	1.51E-07
IL36RN	2.70E-08
IL4I1	7.72E-07
IL6	2.16E-08
INMT	4.74E-06
INSL5	0.004558
IPO5P1	9.64E-12
IQCD	2.24E-05
IQCH	0.001029
IQCK	4.94E-07
IQUB	2.72E-05
IRF8	0.000665
IRX5	1.83E-12
ISL1	2.56E-12
ISL2	3.42E-11
ITGA7	3.55E-05

ITGA8	1.10E-07
ITGB2	4.17E-05
ITGBL1	0.00186
ITIH5	7.53E-06
ITLN1	0.006835
ITM2A	5.08E-06
IVL	1.87E-06
IYD	5.54E-08
JAM2	1.21E-05
JAM3	0.001238
JPH2	2.20E-06
KBTBD12	1.94E-06
KCNA4	1.05E-05
KCNA5	0.000209
KCNB1	1.71E-12
KCNC1	4.40E-06
KCNE1	0.000112
KCNH6	7.03E-07
KCNJ1	5.70E-07
KCNJ10	2.36E-05
KCNJ16	2.17E-05
KCNK10	2.57E-05
KCNK3	6.78E-05
KCNMA1	0.002529
KCNMB2	0.000175
KCNMB2-AS1	0.000412
KCNN3	1.91E-06
KCNRG	5.18E-05
KCTD14	1.10E-05
KCTD16	3.20E-07
KHDRBS2	4.26E-09
KIAA0101	6.44E-11
KIAA1211L	4.91E-06
KIAA1324	1.31E-12
KIAA1456	1.82E-06
KIAA1524	3.48E-08
KIAA1549L	1.52E-08
KIAA2022	2.33E-14
KIF11	1.87E-09
KIF14	7.88E-11

KIF15	3.75E-08
KIF18A	9.02E-08
KIF19	2.49E-05
KIF20A	6.93E-06
KIF20B	0.000213
KIF23	5.42E-11
KIF26B	1.46E-07
KIF2C	3.01E-09
KIF3C	3.40E-06
KIF4A	3.69E-09
KIF6	7.43E-05
KIF9	1.35E-05
KIFC1	4.59E-09
KLC3	1.29E-06
KLF15	3.38E-11
KLF3-AS1	2.18E-09
KLHDC1	7.06E-10
KLHDC8A	9.61E-07
KLHDC9	2.20E-06
KLHL32	9.84E-05
KLHL41	4.45E-07
KLK11	1.02E-05
KLK7	0.004085
KLK8	2.29E-05
KNDC1	0.000281
KNL1	1.16E-09
KNTC1	8.44E-12
KPNA2	5.44E-11
KRT16	1.07E-10
KRT16P3	1.04E-08
KRT17	3.80E-05
KRT222	1.10E-10
KRT24	0.013974
KRT27	0.000148
KRT34	5.55E-05
KRT4	0.000359
KRT6B	4.00E-12
KRT6C	3.68E-10
KRT75	1.88E-05
KRT79	3.40E-06

KRT80	3.27E-05
KRTAP19-1	0.002234
KRTAP4-1	5.89E-11
KRTDAP	0.000863
KYNU	4.41E-09
LAD1	3.33E-07
LAIR1	4.93E-06
LAPTM4B	2.02E-08
LAPTM5	2.62E-07
LARP6	3.65E-10
LCA5	6.49E-06
LCA5L	2.30E-05
LCAL1	4.54E-09
LCE3A	0.000207
LCE3D	0.000285
LDB3	7.91E-10
LDHA	1.68E-06
LDLRAD1	1.60E-06
LEPR	3.15E-08
LGI1	0.000154
LGR6	2.00E-13
LHFP	7.61E-05
LHX2	1.14E-11
LIFR	2.76E-08
LIFR-AS1	2.89E-11
LILRA2	4.09E-08
LILRA3	7.39E-07
LILRA4	5.96E-08
LILRA5	6.56E-06
LILRB1	1.78E-06
LILRB2	8.05E-06
LILRB3	3.52E-09
LILRP2	4.73E-09
LIMCH1	7.96E-13
LINC00116	0.000131
LINC00261	1.33E-05
LINC00326	0.000508
LINC00470	0.01955
LINC00479	1.52E-06
LINC00491	6.53E-06

LINC00589	0.000402
LINC00675	4.95E-05
LINC00689	0.013066
LINC00839	1.47E-06
LINC00844	0.000164
LINC00886	1.80E-08
LINC00942	9.93E-06
LINC00968	0.0001
LINC00982	4.21E-10
LINC01094	8.78E-10
LINC01140	1.53E-07
LINC01206	0.001785
LINC01296	5.93E-07
LINC01315	1.75E-14
LINC01354	3.22E-07
LINC01615	2.08E-07
LIPG	1.16E-08
LMNB1	1.26E-06
LMO3	4.50E-07
LMOD1	2.80E-07
LMOD3	0.000555
LOC100287221	2.37E-08
LOC100287357	3.91E-06
LOC100288798	2.76E-05
LOC100506990	3.70E-09
LOC100507311	8.19E-15
LOC100507387	3.40E-06
LOC100507537	0.000404
LOC101927746	6.73E-05
LOC101928045	4.46E-05
LOC101928303	1.69E-08
LOC101928907	4.71E-05
LOC105379239	1.92E-05
LOC149351	2.41E-07
LOC284244	1.19E-09
LOC284344	0.000275
LOC349160	3.07E-06
LOC400710	4.64E-06
LOC401052	9.14E-05
LOC440173	1.04E-05
LOC642484	9.21E-06

LOC728175	7.32E-06
LOC729603	1.75E-06
LOC729970	6.80E-07
LONRF2	3.20E-08
LOR	0.000487
LOXL2	2.05E-06
LPCAT1	5.53E-10
LPO	0.03489
LRCH2	0.001297
LRIG1	2.27E-10
LRP2BP	7.54E-06
LRP8	1.85E-07
LRRC15	1.38E-06
LRRC18	5.33E-07
LRRC2	3.56E-08
LRRC25	1.57E-05
LRRC31	1.99E-06
LRRC34	4.31E-05
LRRC36	2.61E-05
LRRC43	0.000132
LRRC46	8.74E-06
LRRC49	7.33E-07
LRRC4C	3.14E-09
LRRC6	7.46E-05
LRRC71	4.76E-06
LRRC73	6.83E-06
LRRC74B	8.52E-05
LRRIQ1	0.000146
LRRIQ3	0.002349
LRTOMT	5.62E-06
LSAMP	0.000993
LTF	0.033763
LTK	6.02E-08
LUM	0.001165
LURAP1	1.02E-12
LY6H	1.76E-05
LY6K	1.89E-08
LYPD3	9.52E-06
LZTFL1	1.01E-05
MAATS1	1.75E-05

MAB21L3	6.40E-05
MACROD2	6.65E-11
MAD2L1	2.11E-10
MAGEA12	2.19E-05
MAGEA2B	1.40E-05
MAGEA4	9.09E-05
MAGEA9	0.008956
MAGEB2	0.000501
MAGEC1	8.38E-05
MAGED4B	5.23E-07
MAGI2-AS3	1.34E-08
MAGIX	9.07E-08
MAK	0.000466
MALL	6.53E-05
MAMDC2	9.97E-06
MAN1C1	4.64E-12
MAOB	1.16E-07
MAP3K19	2.88E-05
MAPK12	3.62E-06
MAPK4	1.25E-07
MAPK6	1.26E-05
MARCH1	1.04E-05
MARCO	0.000387
MASTL	4.02E-09
MB	1.13E-09
MCEMP1	1.28E-05
MCM10	5.45E-11
MCM2	2.42E-12
MCM4	1.10E-09
MDGA1	1.04E-07
ME1	4.26E-06
ME3	7.96E-13
MEIS3P1	6.75E-14
MELK	4.78E-11
MELTF	6.55E-10
MEOX2	9.56E-07
MEST	1.25E-07
METTL7A	7.20E-13
MEX3B	0.000388
MFAP4	1.60E-06

MFSD4A	9.96E-14
MGAT3	6.33E-07
MGP	1.48E-06
MIA	3.04E-05
MICU3	5.28E-08
MIR503HG	1.47E-08
MIR99AHG	6.64E-11
MITF	6.95E-09
MKI67	1.92E-07
MKL2	1.40E-11
MKRN3	0.005596
MLK4	6.71E-07
MLLT11	1.09E-07
MLPH	1.28E-05
MMP1	7.04E-11
MMP10	0.025007
MMP11	1.27E-10
MMP12	3.59E-11
MMP13	0.015283
MMP3	1.09E-10
MMP9	1.01E-07
MMS22L	3.59E-05
MND1	1.68E-09
MNS1	0.000578
MORN1	6.67E-07
MORN5	8.31E-07
MPDZ	5.67E-07
MPL	6.40E-10
MPP3	2.79E-11
MPPED1	0.000249
MPV17L	8.78E-05
MREG	5.66E-10
MRGPRF	6.72E-05
MROH7	9.82E-10
MROH8	7.35E-09
MROH9	0.000923
MRVI1	0.001109
MS4A4A	0.000245
MS4A8	2.61E-08
MSC	2.10E-11

MSLN	2.66E-07
MSMB	1.90E-06
MSR1	1.24E-05
MSRB3	0.000607
MT1E	1.30E-07
MT1M	6.40E-08
MT3	2.45E-06
MTFR2	4.46E-10
MTHFD1L	2.32E-09
MTHFD2	1.13E-08
MTHFD2P1	5.83E-05
MTURN	2.05E-07
MUC15	2.64E-06
MUC16	5.73E-09
MUC5AC	3.62E-07
MUC7	0.028852
MYBL2	2.12E-13
MYC	4.71E-08
MYCBPAP	2.61E-05
MYH11	1.14E-05
MYLK	0.000167
MYLK2	8.63E-09
MYO10	2.20E-05
MYO15A	4.66E-07
MYO5C	2.39E-12
MYO7A	3.65E-07
MYOC	1.36E-09
MYOM1	1.21E-07
MYOM2	4.70E-08
MYOT	1.47E-13
MYOZ2	2.25E-06
MYOZ3	4.19E-06
MYRIP	1.61E-10
NABP1	4.47E-11
NAMPT	1.45E-12
NAP1L3	0.0004
NAT8L	6.88E-06
NAV2	3.64E-06
NBEA	5.24E-09
NCAPG	1.24E-10

NCAPH	3.52E-09
NCKAP1L	3.36E-06
NCR1	9.23E-05
NDC80	7.97E-09
NDN	3.73E-06
NDNF	2.83E-09
NDRG1	7.05E-09
NDRG4	3.49E-07
NECAB1	5.70E-08
NEFL	3.04E-08
NEFM	0.000547
NEGR1	0.000147
NEIL3	1.84E-08
NEK10	0.0001
NEK2	3.44E-07
NEMP1	4.53E-08
NETO2	1.32E-08
NEURL3	5.34E-12
NFIA	5.06E-12
NFIB	8.08E-11
NHLRC4	1.15E-05
NIPA1	6.66E-07
NKAIN1	0.00014
NKX2-1	1.75E-11
NKX3-1	0.000151
NLN	9.26E-11
NLRC4	2.58E-05
NLRP7	0.000336
NME5	9.38E-07
NME9	1.66E-06
NMRAL1P1	1.64E-09
NMUR1	1.28E-05
NOSTRIN	1.01E-05
NOX4	8.71E-05
NPAS3	8.46E-05
NPC1	8.30E-11
NPHP1	3.37E-05
NPL	1.46E-11
NPPC	0.000465
NPR3	0.000937

NR2E3	7.42E-06
NR2F1	2.25E-08
NR2F2	1.61E-14
NR2F2-AS1	3.46E-13
NR3C2	2.02E-16
NRAP	4.15E-08
NRG2	3.83E-15
NRIP3	5.45E-08
NRXN1	0.000507
NRXN3	2.90E-09
NSUN7	1.64E-06
NTF3	1.46E-06
NTN1	4.89E-13
NTRK2	5.69E-06
NTRK3	5.97E-08
NUCB2	3.17E-09
NUDT10	1.87E-05
NUDT11	0.00069
NUDT9P1	1.08E-08
NUF2	2.23E-11
NUSAP1	2.01E-11
NXPE2	0.033038
NXPH3	4.42E-08
OBFC1	1.65E-14
ODAM	0.014332
OGN	2.80E-07
OIP5	1.28E-10
OMD	0.005553
ONECUT2	0.000592
OR2B6	1.53E-06
ORC1	2.58E-08
ORC6	2.11E-10
ORM1	5.34E-12
OSBPL6	0.001496
OSCP1	1.64E-06
OSM	8.35E-08
OSMR	1.79E-07
OTUB2	1.94E-05
OVOS2	3.99E-09
OXTR	0.000344

P2RX5	1.38E-06
PACRG	4.55E-06
PAQR5	0.000332
PARPBP	1.77E-10
PARVB	1.15E-07
PAX9	1.05E-08
PBK	6.84E-08
PCAT7	1.28E-07
PCDH10	0.000154
PCDH20	4.80E-10
PCDH9	8.73E-07
PCDHA11	6.89E-08
PCSK1	2.29E-06
PCSK2	4.26E-07
PCSK9	8.82E-10
PDE11A	0.000132
PDE1A	6.20E-09
PDE2A	2.46E-07
PDE5A	2.72E-08
PDE6B	1.12E-07
PDE8B	5.84E-05
PDK1	1.30E-05
PDK4	8.02E-09
PDZD2	4.61E-10
PDZRN3	4.52E-05
PDZRN4	6.78E-05
PEBP4	3.34E-05
PENK	0.003304
PER3	3.86E-07
PF4V1	0.00837
PFKFB4	5.06E-12
PGA3	1.65E-06
PGAM2	4.15E-06
PGAM5	2.25E-09
PGBD5	1.24E-06
PGD	5.70E-06
PGF	1.45E-09
PGLYRP4	1.12E-06
PGM5	1.93E-10
PGM5P4-AS1	2.69E-09

PGR	3.11E-08
PHYHD1	3.48E-14
PHYHIP	1.78E-10
PI16	1.74E-09
PI3	0.001758
PID1	5.76E-09
PIF1	3.07E-10
PIF0	6.75E-07
PIGR	1.45E-08
PIGX	1.50E-11
PIH1D2	3.28E-05
PIH1D3	1.09E-05
PIP	0.000982
PIP5K1B	3.57E-08
PITX2	0.001323
PKMYT1	2.26E-11
PKP1	1.18E-06
PLA2G10	4.67E-07
PLA2G7	2.25E-09
PLAC1	5.30E-07
PLAC8	1.52E-05
PLAT	5.28E-05
PLAU	9.05E-12
PLAUR	4.16E-12
PLCB4	1.06E-09
PLCD4	3.61E-09
PLCE1	4.77E-12
PLEK	5.77E-05
PLEKHA6	1.47E-09
PLEKHB1	7.68E-07
PLEKHH2	6.18E-11
PLEKHS1	1.20E-09
PLK1	1.39E-09
PLK4	1.30E-05
PLN	2.26E-07
PLP1	2.13E-07
PLPP4	2.16E-08
PLPPR3	1.40E-06
PMCH	0.010107
PMP2	6.53E-07

PNMAL1	0.000186
PNPLA3	7.24E-06
PODXL2	0.000277
POLE2	2.65E-07
POLQ	3.78E-10
POM121	1.67E-06
POPDC3	9.70E-07
POU3F1	0.000154
POU4F1	5.91E-06
POU6F2	2.88E-08
PPARGC1A	1.26E-09
PPAT	1.07E-06
PPIF	3.87E-08
PPIL6	8.19E-06
PPM1L	6.38E-11
PPP1R12B	7.02E-07
PPP1R14A	0.000115
PPP1R17	0.024345
PPP1R1A	9.03E-08
PPP1R1B	0.004432
PPP1R32	2.80E-05
PPP1R36	3.89E-08
PPP1R3C	3.25E-09
PPP1R9A	3.40E-06
PPP2R2C	1.41E-09
PRAME	3.09E-11
PRB1	0.003682
PRB2	0.009571
PRB3	0.00315
PRB4	0.006996
PRC1	1.62E-10
PRDM13	1.43E-09
PRDM16	4.85E-14
PRELP	2.56E-05
PRG4	0.036625
PRH2	0.006323
PROK2	0.001918
PROM1	0.000157
PROS1	0.000325
PRPH2	1.84E-05

PRR15	4.02E-09
PRR15L	7.01E-09
PRR29	1.21E-05
PRR4	0.020411
PRRT3	1.35E-07
PRSS2	0.002627
PRSS23	9.07E-11
PRSS3	0.000434
PRUNE2	2.87E-09
PSCA	9.08E-05
PSG6	0.000204
PSTPIP2	3.32E-05
PTCHD1	0.029589
PTGFR	2.14E-09
PTGIS	6.42E-06
PTGS2	0.001076
PTHLH	7.78E-09
PTPRN2	9.00E-10
PTPRO	2.16E-05
PTPRT	3.15E-07
PTTG2	1.16E-05
PTTG3P	3.47E-06
PVR	1.18E-06
PXDN	9.34E-05
PZP	4.14E-05
RAB36	0.00023
RAB37	1.73E-08
RAB42	3.93E-08
RAC2	2.78E-11
RACGAP1	2.70E-08
RACGAP1P	4.03E-09
RAD51	1.36E-13
RAD51AP1	1.53E-11
RAD54L	1.27E-12
RAI2	6.87E-08
RAMP1	3.92E-06
RASGRP1	4.15E-05
RASL12	1.27E-05
RASSF6	2.50E-07
RBL1	1.76E-06

RBM24	5.40E-05
RBMS3	1.07E-10
RCAN2	1.22E-06
RCCD1	5.15E-12
RDM1	8.17E-07
RECQL4	1.38E-11
RECQL5	7.47E-05
REEP1	9.58E-08
RELT	2.12E-13
RERG	2.00E-07
RERGL	1.02E-07
RFC4	2.12E-13
RFX2	5.11E-06
RGMB-AS1	6.08E-06
RGN	1.02E-09
RGS17	4.80E-06
RGS20	1.15E-08
RGS22	2.16E-06
RGS5	4.77E-05
RGS6	8.14E-06
RHCG	0.000591
RHOF	2.88E-06
RHOJ	0.000132
RIBC2	5.15E-05
RIC3	1.83E-14
RIMS4	2.79E-06
RIT1	3.56E-12
RMI2	3.36E-08
RNASE2	1.10E-06
RNASE4	1.19E-08
RNASE7	0.000332
RNF17	0.000517
RNF212	9.21E-06
ROPN1	3.38E-06
ROPN1B	1.50E-08
ROPN1L	3.93E-06
ROR1	6.49E-05
RORC	1.00E-06
RP1	0.000253
RPL15	3.45E-10

RPRML	1.34E-05
RPTN	0.013676
RRAD	7.60E-05
RRM2	2.29E-09
RSPH1	2.24E-05
RSPH10B	6.56E-06
RSPH14	4.71E-06
RSPH4A	2.79E-06
RSPH9	1.07E-05
RSPO1	3.11E-05
RSRC1	6.68E-12
RTKN2	0.00018
RUNDC3B	3.31E-06
RUNX1T1	0.000488
RYR2	0.002303
RYR3	0.000871
S100A12	4.26E-06
S100A2	0.000456
S100A7	3.15E-08
S100A7A	9.27E-05
S100A8	1.70E-07
S100A9	1.18E-07
S100P	0.000188
SAMSN1	5.73E-05
SAPCD2	1.14E-09
SAXO2	5.11E-06
SBSPON	1.96E-08
SCARA5	6.89E-09
SCARB1	7.96E-06
SCD	3.37E-10
SCGB1A1	2.41E-07
SCGB2A1	2.55E-06
SCGB3A1	4.01E-09
SCGN	2.14E-09
SCN2B	7.78E-12
SCN3A	8.60E-07
SCN7A	1.92E-11
SCN9A	1.45E-05
SCRG1	1.53E-05
SDPR	7.06E-10

SDR16C5	9.63E-08
SDS	1.27E-05
SEC14L3	1.81E-06
SELENBP1	2.00E-13
SEMA3E	4.02E-06
SEMA5A	4.68E-10
SEMA7A	6.70E-06
SENP2	2.11E-10
SENP5	6.54E-13
SERPINA5	0.000463
SERPINA6	0.00042
SERPINB10	2.99E-07
SERPINB11	0.000126
SERPINB2	0.016183
SERPINB3	0.003539
SERPINB5	0.000267
SERPINB9	7.52E-06
SERPINE1	7.04E-10
SERPINI2	2.60E-05
SFN	1.80E-07
SFRP1	0.000875
SFRP4	0.006285
SFTA3	1.02E-12
SGCA	2.80E-06
SGO1	6.46E-08
SGSM1	1.13E-10
SGTB	2.88E-06
SH2D1B	0.006211
SH2D5	2.74E-10
SH3BGRL2	1.63E-10
SHANK2	1.07E-06
SHCBP1	2.76E-09
SHISA6	3.25E-07
SHOX2	3.36E-06
SIGLEC5	8.66E-05
SIGLEC7	4.92E-05
SIGLEC9	1.22E-05
SIM2	0.000119
SIRPA	0.000101
SIRPB1	5.73E-07

SKA1	2.14E-08
SKA3	6.93E-09
SKIDA1	5.71E-09
SKP2	5.28E-12
SLAMF8	0.000185
SLC11A1	1.08E-08
SLC12A2	2.01E-05
SLC12A8	2.41E-09
SLC13A3	5.88E-07
SLC14A2-AS1	0.000244
SLC16A1	1.61E-10
SLC16A10	4.14E-06
SLC16A12	1.19E-07
SLC16A9	7.93E-09
SLC19A1	2.12E-13
SLC1A2	0.002959
SLC1A3	0.000712
SLC22A16	0.000791
SLC22A3	0.000605
SLC22A4	5.46E-06
SLC23A1	9.62E-07
SLC24A2	0.000626
SLC25A21-AS1	6.13E-10
SLC27A2	4.84E-05
SLC27A4	5.12E-07
SLC27A6	0.001263
SLC2A1	3.49E-09
SLC2A3	4.28E-05
SLC2A4	0.001259
SLC2A5	8.69E-08
SLC30A3	9.67E-09
SLC35F1	9.37E-07
SLC35F3	0.000524
SLC39A2	6.96E-08
SLC3A2	2.81E-08
SLC44A4	4.66E-06
SLC47A2	0.000148
SLC4A4	1.37E-06
SLC4A8	2.20E-06
SLC51B	2.71E-05

SLC5A1	5.20E-05
SLC5A8	0.006707
SLC6A10P	5.63E-09
SLC7A11	1.14E-06
SLC7A5	2.18E-10
SLC9C2	0.001089
SLCO1A2	0.013369
SLCO3A1	1.18E-08
SLCO4A1	3.14E-07
SLCO4C1	1.82E-10
SLFN13	2.05E-05
SLIT2	1.09E-07
SLITRK3	1.80E-05
SLITRK5	0.000134
SLITRK6	4.96E-14
SLPI	1.78E-08
SMAD9	2.93E-08
SMC4	2.25E-13
SMIM22	1.34E-06
SMIM6	0.000213
SMPD3	5.66E-07
SMPX	2.17E-05
SNX10	8.69E-09
SNX20	0.000169
SNX31	2.26E-07
SNX5	6.20E-12
SOBP	9.02E-12
SOCS3	6.28E-06
SOD2	2.57E-15
SOD3	7.23E-09
SOHLH1	0.001814
SORBS1	5.20E-09
SORBS2	2.47E-10
SORCS1	0.000251
SOST	4.55E-10
SOWAHA	5.34E-06
SOX10	0.000308
SOX11	2.73E-09
SOX2-OT	5.40E-05
SOX5	3.18E-11

SOX8	7.38E-05
SOX9-AS1	9.33E-06
SP5	1.55E-06
SPA17	0.000141
SPACA9	0.000188
SPAG16	0.000127
SPAG17	0.000391
SPAG5	8.96E-09
SPAG6	5.66E-06
SPAG8	8.14E-06
SPARCL1	4.69E-07
SPATA17	0.000333
SPATA18	2.81E-06
SPATA4	5.69E-06
SPATA6	3.15E-11
SPATA6L	3.54E-05
SPATS1	3.22E-05
SPC24	5.88E-08
SPC25	2.20E-09
SPDEF	3.63E-06
SPEF1	6.83E-06
SPEF2	3.52E-05
SPERT	0.000479
SPINK1	0.014376
SPOCD1	3.24E-08
SPOCK3	0.007529
SPP1	8.42E-09
SPRR1A	1.10E-05
SPRR1B	1.85E-07
SPRR2C	4.73E-08
SPRR2D	3.99E-08
SPRR2E	5.96E-06
SPRR2G	1.50E-08
SPRR3	0.001727
SPRY2	4.28E-11
SRD5A2	0.000103
SRI	2.50E-07
SRPX	0.000564
SRXN1	2.97E-09
SSPN	3.60E-07

SSTR1	1.94E-07
SSUH2	7.17E-07
ST3GAL4	4.31E-06
ST6GALNAC1	2.35E-09
STATH	7.28E-05
STC2	1.69E-09
STK33	1.35E-05
STK38L	1.70E-11
STMN1	1.12E-07
STMND1	6.29E-06
STOML3	3.46E-06
STOX1	6.25E-07
STRIP2	2.52E-09
SULT1B1	0.000674
SULT1E1	0.000848
SULT4A1	3.64E-05
SYBU	2.14E-11
SYNC	3.11E-09
SYNDIG1	0.005462
SYNE1	2.61E-08
SYNM	0.000227
SYNPO2	9.32E-08
SYT1	2.51E-05
SYT13	0.000136
SYT14	0.000101
SYTL2	3.84E-07
TACC3	1.49E-11
TAGAP	0.000182
TAGLN3	0.000233
TAS1R1	8.14E-08
TBX2	6.31E-05
TBX5	0.000902
TCAF2	2.33E-07
TCEAL2	9.71E-07
TCF19	1.60E-05
TCF21	1.04E-07
TCL1A	0.000762
TCN1	1.47E-05
TCP11	1.79E-05
TCTE1	2.46E-05

TCTEX1D1	0.000364
TDH	3.66E-06
TDO2	2.04E-06
TEAD2	7.75E-07
TEKT1	0.000219
TEKT2	3.30E-05
TEKT3	0.000703
TEX19	2.50E-08
TEX26	0.001416
TFCP2L1	6.74E-06
TFF1	0.000835
TFF3	1.52E-05
TFRC	2.33E-14
TGM5	2.02E-05
THEMIS2	9.30E-08
THSD4	4.37E-09
TICRR	1.35E-12
TIMD4	0.003601
TIMELESS	2.09E-13
TIMP3	3.13E-07
TK1	1.03E-12
TLE2	2.01E-12
TLR6	8.62E-09
TLR8	4.39E-05
TM4SF19	5.47E-10
TM4SF4	0.000231
TMC5	7.29E-06
TMC05A	3.04E-06
TMEFF1	9.26E-07
TMEFF2	0.001
TMEM100	1.99E-08
TMEM108	0.000116
TMEM125	7.72E-09
TMEM133	7.93E-09
TMEM139	0.000293
TMEM150C	4.17E-08
TMEM155	0.009696
TMEM158	3.43E-05
TMEM163	1.69E-09
TMEM178A	1.04E-08

TMEM190	0.000383
TMEM213	2.79E-09
TMEM220	1.32E-08
TMEM232	5.85E-05
TMEM47	3.22E-06
TMEM61	1.22E-11
TMEM81	3.40E-05
TMPRSS11A	0.019765
TMPRSS11B	0.010798
TMPRSS11E	5.12E-07
TMPRSS11F	7.11E-05
TNFAIP6	5.31E-06
TNFRSF19	2.88E-09
TNFRSF9	1.16E-10
TNFSF11	1.37E-05
TNFSF9	9.39E-11
TNIP3	3.88E-07
TNN	0.006793
TNNC1	5.73E-12
TNNT1	2.00E-08
TNNT3	0.000206
TNXB	7.53E-10
TONSL	1.01E-11
TOP2A	1.49E-08
TPM4	2.32E-11
TPPP3	1.95E-05
TPX2	1.64E-09
TRABD2B	1.78E-08
TRAF3IP2-AS1	3.23E-06
TREM1	4.46E-07
TREML2	1.34E-06
TRIB3	9.58E-09
TRIM59	4.91E-06
TRIM63	5.89E-07
TRIP13	1.74E-09
TROAP	1.32E-12
TRPA1	9.25E-07
TRPC1	4.73E-10
TRPM2	4.70E-05
TRPV6	8.33E-11

TSGA10	1.06E-05
TSLP	7.01E-07
TSNAXIP1	2.47E-05
TSPAN1	1.52E-07
TSPAN12	2.78E-11
TSPAN2	1.10E-06
TSPAN8	2.47E-10
TSPOAP1	9.04E-09
TTC16	5.99E-05
TTC21A	4.41E-05
TTC23L	5.85E-05
TTC25	0.000154
TTC29	1.76E-05
TTK	1.01E-10
TTL	6.58E-07
TTLL6	0.000544
TTR	0.004307
TTTY14	0.014969
TTYH2	0.000103
TTYH3	5.34E-12
TUBA1C	1.22E-11
TUBB3	6.29E-12
TUBB4A	7.17E-10
TUBB6	3.04E-06
TUSC3	4.49E-05
TXLNB	0.000139
TYMS	4.68E-09
TYMSOS	2.35E-05
UBE2C	1.08E-10
UBE2S	1.53E-10
UBE2T	5.71E-11
UBE3C	1.63E-08
UBXN10	3.35E-06
UCA1	8.10E-05
UCHL1	1.14E-06
UG0898H09	0.000115
UGT1A8	0.000165
UGT2A1	1.01E-07
UGT2B10	3.96E-05
UGT2B11	0.000375

UGT2B7	3.23E-05
UHRF1	9.44E-11
ULBP2	7.78E-07
UMPS	3.14E-07
UNC45B	0.00012
UPP1	1.11E-08
USH1G	1.73E-05
USP2	2.06E-05
VCX	1.74E-06
VCX2	1.03E-06
VCX3A	1.39E-06
VCY	1.06E-06
VEGFA	5.44E-11
VILL	1.93E-10
VIPR1	5.23E-07
VIT	1.25E-10
VSIG2	1.69E-08
VSTM2L	3.06E-09
VWA3A	0.003027
VWA3B	4.27E-05
WASF1	8.14E-10
WDFY3-AS2	8.17E-11
WDHD1	2.65E-12
WDR38	2.72E-05
WDR49	3.85E-06
WDR63	2.48E-05
WDR72	8.52E-09
WDR78	1.01E-06
WDR86-AS1	2.11E-05
WFDC1	4.63E-09
WFDC2	1.46E-08
WFDC6	4.58E-07
WIF1	0.001362
WISP1	1.76E-06
WISP2	2.40E-06
WNT2	1.97E-08
XCL1	2.25E-05
XCL2	7.68E-06
XDH	5.88E-05
XKR4	6.00E-09

XKR6	2.73E-08
XRCC2	4.76E-11
ZBBX	9.07E-06
ZBED2	0.000107
ZBTB16	2.02E-08
ZC2HC1C	8.02E-06
ZCCHC5	0.000238
ZDHHC15	4.53E-08
ZFP2	3.47E-11
ZFP64	2.56E-12
ZFPM2	4.96E-05
ZG16B	7.92E-05
ZIC2	1.22E-08
ZIC5	9.75E-10
ZIM2	1.13E-05
ZKSCAN7	1.99E-07
ZMYND10	1.19E-05
ZMYND12	2.58E-06
ZNF107	9.96E-06
ZNF114	3.56E-07
ZNF132	7.35E-09
ZNF214	4.25E-05
ZNF295-AS1	0.001865
ZNF300P1	1.84E-07
ZNF385D	0.001332
ZNF396	2.53E-05
ZNF415	2.66E-09
ZNF471	5.75E-07
ZNF519	2.66E-05
ZNF540	6.56E-16
ZNF608	2.02E-10
ZNF623	1.59E-06
ZNF695	4.30E-05
ZNF704	1.25E-10
ZNF781	3.51E-06
ZP3	1.49E-05
ZSCAN18	4.73E-10
ZWINT	6.31E-11